DENV NS1 and MMP-9 cooperate to induce vascular leakage by altering endothelial cell adhesion and tight junction

Geng Li[1,3,4#], Pan Pan[1, 2#], Miaomiao Shen[3], Zhenyang Yu[3], Weiwei Ge[3], Zizhao Lao[4], Yaohua Fan[4], Keli Chen[3], Zhihao Ding[3], Wenbiao Wang[1], Pin Wan[1], Muhammad Adnan Shereen[3], Zhen Luo[1], Xulin Chen[1], Qiwei Zhang[1], Luping Lin[4,5]* and Jianguo Wu[1,2,3]*

[1]Guangdong Provincial Key Laboratory of Virology, Institute of Medical Microbiology, Jinan University, Guangzhou 510632, China. [2]The first Affiliated Hospital of Jinan University, Guangzhou 510632, China. [3]State Key Laboratory of Virology, College of Life Sciences, Wuhan University, Wuhan 430072, China. [4]Center for Animal Experiment, Guangzhou University of Chinese Medicine, Guangzhou 510405, China. [5]Guangzhou Eighth People's Hospital, Guangzhou 510000, China.

[#]These authors contributed equally to this work

***Correspondence Authors**: Jianguo Wu, Institute of Medical Microbiology, Jinan University, Guangzhou 510632, China, Tel.: +86-20-85226420, Fax: +86-20-85226420, Email: jwu898@jnu.edu.cn; Luping Lin, Email: linlupingdoctor@qq.com

Short title: NS1 and MMP-9 together induce vascular leakage

Word counts for Abstract: 250

Word count for the author summary: 178

Abstract

Dengue virus (DENV) is a mosquito-borne pathogen that causes a spectrum of diseases including life-threatening dengue hemorrhagic fever (DHF) and dengue shock syndrome (DSS). Vascular leakage is a common clinical crisis in DHF/DSS patients which is closely associated with increased endothelial permeability. The presence of vascular leakage causes hypotension, circulatory failure or disseminated intravascular coagulation as the disease progresses, which can lead to death under such conditions. However, the mechanisms by which DENV infection caused the vascular leakage are not fully understood. This study reveals a distinct mechanism by which DENV induces endothelial permeability and vascular leakage in human endothelial cells and mice tissues. We initially show that DENV2 promotes the matrix metalloproteinase-9 (MMP-9) expression and secretion in DHF patient serum, peripheral blood mononuclear cells (PBMCs) and macrophages, and further reveal that DENV non-structural protein 1 (NS1) induces MMP-9 expression through activating the nuclear factor κB (NF-κB) signaling pathway. Additionally, NS1 inhibits TIMP-1 expression to facilitates the MMP-9 enzymatic activity which alters the adhesion and tight junctions and vascular leakage in human endothelial cells and mouse tissues. Moreover, NS1 recruits MMP-9 to interact with β-catenin and Zona occludins protein-1/2 to degrade the important adhesion and tight junction proteins, thereby inducing endothelial hyperpermeability and vascular leakage in human endothelial cells and mouse tissues. Thus, we reveal that DENV NS1 and MMP-9 cooperatively induce vascular leakage by impairing endothelial cell adhesion and tight junction, and suggest that MMP-9 may serve as a potential target for the treatment of hypovolemia in DSS/DHF patients.

Author Summary

DENV is the most common mosquito-transmitted viral pathogen in humans. In general, DENV-infected patients are either asymptomatic or have flu-like symptoms with fever and rash. However, in severe cases of DENV infection, the disease may progress to dengue hemorrhagic fever (DHF) or dengue shock syndrome (DSS), the leading causes of morbidity and mortality in school-age children in tropical and subtropical regions. DENV-induced vascular leakage is characterized by enhanced vascular permeability without morphological damage to the capillary endothelium. We found that a distinct mechanism of DENV NS1 and MMP-9 cooperatively induce vascular leakage is the main reason leading to death in severe dengue patients. Also, NS1 recruits MMP-9 to degrade β-catenin, ZO-1, ZO-2 to intervene endothelial hyperpermeability in human endothelial cells and mouse vascular. Finally, we reveal that DENV activating NF-κB signaling pathway induces MMP-9 expression, in patients, mice, PBMC and macrophages though the viral NS1 protein. This study would provide new in signs into the pathogenesis caused by DENV infection, and suggest that MMP-9 may acts as a drug target for the prevention and treatment of DENV-associated diseases.

Keywords: DENV NS1; MMP-9; vascular leakage; endothelial cell adhesion; tight junctions

Introduction

Dengue virus (DENV) is the most common mosquito-transmitted viral pathogen in humans. As reported by the World Health Organization (WHO), an estimated 40% of the world population is at risk of DENV infection, and approximately 390 million people worldwide are infected with DENV every year [1–3]. As mosquitoes are moving to new areas because of a climate change, the disease is spreading to less tropical and more temperate countries, and the WHO has named dengue as one of the world's top 10 threats to global health in 2019 [4]. In general, DENV-infected patients are either asymptomatic or have flu-like symptoms with fever and rash. However, in severe cases of DENV infection, the disease may progress to dengue hemorrhagic fever (DHF) or dengue shock syndrome (DSS), the leading causes of morbidity and mortality in school-age children in tropical and subtropical regions [1, 5]. According to the latest WHO classification, dengue severity is divided into dengue without warning signs, dengue with warning signs, and severe dengue. vascular leakage, as one of the key features of DHF/DSS or severe dengue, is closely associated with increased vascular permeability in DENV-infected patients [6]. The presence of vascular leakage causes hypotension, circulatory failure or disseminated intravascular coagulation as the disease progresses, which can lead to death under such conditions. So far, there is no licensed antiviral treatment but supportive therapy, e.g., fluid management, available for patients with vascular hyperpermeability as the mechanism underlying the phenomenon remains unclear.

DENV-induced vascular leakage is characterized by enhanced vascular permeability without morphological damage to the capillary endothelium. Despite the findings on DENV replication in some human endothelial cells (ECs), results from the postmortem analysis of DENV-infected human

tissues indicate no generalized DENV EC infection, which is supported by the fact that patients with severe DENV infection manage to fully recover in a short time [7]. All evidence that the loss of vascular integrity and function in DENV infection *in vivo* is not caused by extensive damage to the endothelium. Instead, vasoactive endothelial factors released from DENV-infected cells appear to play a major role in this phenomenon. During DENV infection, viruses mainly target at monocytes/macrophages and dendritic cells (DCs) for replication *in vivo*. Changes in production of interleukin-1 (IL-1), interleukin-6 (IL-6), macrophage inhibitory factor (MIF), tumor necrosis factor α (TNF-α), and metalloproteinases are noted in macrophages and DCs infected with DENV *in vitro* [8, 9]. In a study of EC barrier function using *in vitro* models to describe movement of labeled macromolecules or changes in cell electrical resistance, it was demonstrated that soluble factors released from DENV-infected macrophages could change the permeability of an EC monolayer in the absence of relevant viral-induced cytopathic effect [10]. Taken together, altered production of factors released from circulating monocytes, macrophages, or DCs in human tissues occurs during DENV infection, and these factors may coordinate to induce functional changes in endothelial cells.

The maintenance of endothelial cell permeability is mainly determined by two factors. One is the polyglycoprotein complex that forms a protective membrane on the cell surface to ensure the integrity of endothelial cells [11, 12]. The other is the adhesion and tight junction between endothelial cells, which play important roles in maintaining the integrity of endothelial cells [13]. In addition to promoting cell adhesion, the adhesion and tight junctions can also regulate cell growth, apoptosis, gene expression, and cardiovascular formation by altering intracellular signals [13]. The adhesion and tight junction proteins play important roles in maintaining homeostasis. There are two major types of junction, adhesion junction and tight junction [13]. The changes in adhesion and tight

104 junction structures are regulated by matrix metalloproteinases (MMPs), which are destructive to the
105 integrity of endothelial cells [14]. In the MMP family, the MMP-9 protein specifically degrades
106 extracellular matrix to promote tumor migration [15, 16]. Although previous study reported that
107 DENV induces vascular leakage by up-regulating the expression of MMP-9 in Dendritic cells (DCs)
108 [17], the specific mechanism underlying this regulation is not clear.

109 Endothelial glycocalyx has been shown to increase endothelial permeability through
110 degradation. Under normal physiological conditions, the glycocalyx controls a number of
111 physiological processes as a barrier, which, particularly, prevents leukocytes and platelets from
112 adhering to vessel walls [18]. Besides, the degradation of the glycocalyx is closely related to severe
113 vascular leakage in DENV infections. However, it is not fully understood what the causes of
114 glycocalyx degradation are during DENV infection. DENV non-structural protein 1 (NS1) is an
115 established early diagnostic marker for DENV infection. The serum concentration of NS1 can reach
116 up to 50 μg/ml in a DHF/DSS case, which is shown to be positively correlated with the disease
117 severity. In fact, the role of NS1 in DENV-induced vascular leakage was not described until 2015
118 when DENV NS1-induced vascular leakage was extensively discussed [19]. From a previous study,
119 NS1 induced vascular leakage in mice, and anti-NS1 antibodies played a role in reducing NS1-
120 induced vascular leakage and the mortality rate. However, the NS1 receptor(s) remains controversial.
121 A study suggested that NS1 induced vascular leakage via Toll-like receptor 4 (TLR4) [20]. In
122 another study, it was reported that autophagy-mediated junction disruption was associated with
123 DENV NS1-induced vascular leakage, which may explain why vascular leakage in DENV-infected
124 patients is a rapid and reversible pathogenic change [21]. NS1-induced MIF secretion is involved in
125 NS1-induced EC autophagy. In addition, it was shown in an *in vitro* study that DENV-infected cells

126 increased endothelial permeability by inducing MIF secretion. NS1 not only disrupts endothelial
127 junctions but also causes vascular leakage through HPA-1-mediated glycocalyx degradation. In
128 short, there is growing evidence indicating that NS1 plays a critical role in dengue pathogenesis as it
129 causes vascular leakage and hemorrhage during DENV infection [22]. Vascular permeability
130 changes can be induced by destroying the thin (about 500 nm) and gel-like endothelial glycocalyx
131 layer (EGL) that coats the luminal surface of blood vessels [23, 24]. Although vascular permeability
132 changes are the main research focus, the specific mechanism underlying DENV pathogenesis needs
133 to be further investigated.

134 In the present study, we reveal a distinct mechanism by which DENV induces endothelial
135 permeability and vascular leakage in human endothelial cells and mouse tissues. DENV2 infection
136 induces MMP-9 expression and secretion in human PBMCs and macrophages through NS1-induced
137 activation of the NF-κB signaling pathway. More interestingly, NS1 also interacts with MMP-9,
138 resulting in degradation of important adhesion and tight junction proteins, imparing the adhesion and
139 tight junctions, and consequently inducing endothelial hyperpermeability and increasing vascular
140 leakage in human endothelial cells and mouse tissues. Collectively, these findings demonstrate that
141 NS1 and MMP-9 opt to cause endothelial hyperpermeability and vascular leakage by impairing
142 endothelial cell adhesion and tight junctions.

Results

DENV enhances the production of MMP9 and TIMP-1 in severe dengue patients

Previous studies have found that NS1 protein produced during dengue virus infection closely correlated with the onset of disease by promoting vascular leakage. In our study, we found that the concentrations of NS1 protein in the serum samples of severe dengue patients continued increase with the prolongation of the infection time (Fig 1A). Previous studies have found that matrix metalloprotein-9 (MMP-9, also known as Gelatinase B, GelB) produced by DENV-infected dendritic cells could induce vascular leakage and the Tissue Inhibitor of Metalloproteinases-1 (TIMP-1) could inhibit the production of MMP-9. We also found that the concentrations of MMP-9 protein in the serum samples of severe dengue patients increased over the course of DENV infection (Fig 1B). In contrast, the levels of TIMP-1 protein in the serum samples of severe dengue patients gradually decreased (Fig 1C). Statistical analysis showed a close correlation between NS1 and MMP-9 (Fig 1D). However, there was a converse correlation between TIMP-1 and MMP-9 or NS1(Fig 1E and F) in the sera of severe dengue patients. These results suggest that the NS1 and MMP-9 interaction may play an important role in severe dengue patients.

DENV NS1 interacts with MMP-9

To assess DENV protein(s) involved in the regulation of MMP-9 production, we determined the interaction of MMP-9 with the viral proteins. Human embryonic kidney 293T (HEK293T) cells were co-transfected with pHA-MMP-9 and each vector (pFlag-Cap, pFlag-M, pFlag-Prm, pFlag-E, pFlag-NS1, pFlag-NS2A, pFlag-NS2B, pFlag-NS3, pFlag-NS4A, and pFlag-NS4B) expressing individual

166 DENV proteins (Cap, M, Prm, E, NS1, NS2A, NS2B, NS3, NS4A, and NS4B), respectively. Co-
167 immunoprecipitation (Co-IP) assays showed that MMP-9 interacted with DENV NS1 and NS3
168 proteins but not with other viral proteins (Fig 2A). In this study, we primarily focused on NS1 but
169 not NS3 because both MMP-9 and NS1 are secreted proteins [25] and NS1 plays a role in the
170 regulation of vascular leakage upon DENV infection [19]. Co-IP analysis further confirmed that NS1
171 interacted with MMP-9 (Fig 2B). Confocal microscope also showed that NS1 and MMP-9 were co-
172 localized in the cytoplasm of HEK293T cells (Fig 2C). Moreover, the domains of MMP-9 involved
173 in the MMP-9/NS1 interaction were determined by progressive truncation of MMP-9 (D1–D9) (Fig
174 2D, top). HEK293T cells were co-transfected with pHA-NS1 along with each of the plasmids
175 expressing truncated MMP-9 protein, respectively. Co-IP results showed NS1 interacted with MMP-
176 9 D1 (106–707), MMP-9 D4 (106–511), MMP-9 D5 (1–511), MMP-9 D6 (106–440), MMP-9 D7
177 (106–233), MMP-9 D8 (106–397), or MMP-9 D9 (223–440), but not with MMP-9 D2 (440–707) or
178 MMP-9 D3 (512–707), suggesting that the Zinc-binding catalytic domain and the Fibronectin type-
179 like domain D6 (106–440) are involved in MMP-9/NS1 interaction (Fig 2D, bottom). Taken
180 together, the results demonstrate that DENV NS1 interacts with MMP-9.
181
182 **NS1 induces MMP-9 expression through activation of the NF-κB pathway and inhibition of the**
183 **TIMP-1 production**
184 The molecular mechanism by which NS1 regulates MMP-9 expression was investigated. THP-1
185 differentiated macrophages were transfected with pFlag-NS1 plasmid at varying amounts. MMP-9
186 protein production (Fig 3A, top), MMP-9 enzyme activity (Fig 3A, middle), and MMP-9 mRNA
187 transcription (Fig 3A, middle) were enhanced, whereas TIMP-1 protein production (Fig 3A, bottom)

was inhibited by NS1 in a dose-dependent manner in the THP-1 differentiated macrophages. Similarly, MMP-9 protein production (Fig 3B, top) and MMP-9 enzyme activity (Fig 3B, bottom) were facilitated by NS1 in dose-dependent manners in HEK293T cells. The results suggest that DENV NS1 activates MMP-9 production, secretion, and enzyme activity.

It was reported that MMP-9 promoter contains the nuclear factor κB (NF-κB) regulatory elements [16]. Here, the role of the NF-κB binding sequences of MMP-9 promoter in NS1-activated MMP-9 expression was determined. HEK293T cells were co-transfected with NF-κB reporter plasmid and pHA-NS1. Luciferase assays showed that NF-κB-Luc activity was significantly activated by NS1 in HEK293T cells (Fig 3C). Additionally, THP-1 differentiated macrophages were transfected with pHA-NS1 and treated with a specific inhibitor of NF-κB (SC75741). ELISA assays revealed that secreted MMP-9 protein in the cell culture supernatants was repressed by SC75741 (Fig 3D, top), as shown by decreased levels of MMP-9 protein (Fig 3D, middle). Also, the levels of the MMP-9 mRNA were down-regulated by SC75741 (Fig 3D, bottom), suggesting that NF-κB is required for NS1-induced production of MMP-9. Moreover, phosphorylated p65 (p-p65) and phosphorylated IκBα (p-IκBα) were induced by NS1 in THP-1 differentiated macrophages (Fig 3E), Hela cells (Fig 3F), and HEK293T cells (Fig 3G). Collectively, these results suggest that NS1 promotes MMP-9 expression through activating the NF-κB signaling pathway and inhibition of the TIMP-1production.

DENV2 induces MMP-9 expression and secretion in human PBMCs and macrophages but not in HUVECs

MMP-9 is mainly produced in leukocytes and DENV infects leukocytes [26, 27]. Thus, we

initially focused the role of DENV in the regulation of MMP-9 in human peripheral blood mononuclear cells (PBMCs). PBMCs isolated from healthy individuals were infected with DENV2 for different times or at different concentrations. Quantitative RT-PCR (qRT-PCR) showed that MMP-9 mRNA was induced upon DENV2 infection in PBMCs in a time- (S1A Fig, top) and dose-dependent fashion (S1B Fig, top). Gelatin zymography assays revealed that MMP-9 enzyme activity was enhanced by DENV2 infection in PBMCs (S1A and B Fig, middle). Results from qRT-PCR quantification indicate that DENV E gene mRNA was increased during virus infection (S1A and B Fig, bottom). Additionally, the role of DENV in the regulation of MMP-9 was determined in human acute monocytic leukemia cell line (THP-1). Phorbol 12-myristate 13-acetate (PMA)-differentiated THP-1 macrophages were infected with DENV2 for different times or at different inoculum. Similarly, MMP-9 mRNA was up-regulated upon DENV2 infection in DENV-infected THP-1 macrophages in a time- (Fig 4A, top) and dose-dependent fashions (Fig 4B, top). MMP-9 enzyme activity was also enhanced upon DENV2 infection (Fig 4A and B, middle). Viral E mRNA increased in proportion to infection time and inoculum (Fig 4A and B, bottom). Moreover, the levels of MMP-9 protein and DENV2 NS3 protein increased over the course of DENV2 infection (Fig 4A, middle) and correlated with virus inoculum (Fig 4B, middle). Interestingly, the levels of MMP-9 mRNA (Fig 4C and D, top), MMP-9 enzyme activity, and MMP-9 protein (Fig 4C and D, middle) remained unchanged in endothelial HUVECs upon DENV infection (Fig 4C and D, bottom). The ability of DENV replication was initially analyzed and compared in macrophages and endothelial cells. DENV2 E gene mRNA was significantly higher in infected THP-1 differentiated macrophages as compared to that of human umbilical vein endothelial cells (HUVECs) (Fig 4E). Additionally, secreted MMP-9 protein increased in the supernatants of infected THP-1 differentiated macrophages

232 but was undetectable in the supernatants of infected endothelial HUVECs (Fig 4F, top). Similarly,
233 MMP-9 protein was highly expressed in the infected THP-1 macrophages, while modestly elevated
234 in the infected HUVECs (Fig 4F, bottom). Taken together, these results indicate that DENV
235 infection induced MMP-9 secretion in THP-1 differentiated macrophages but not in endothelial cells.
236
237 **NS1 promotes MMP-9-mediated endothelial hyperpermeability in human cells and mouse**
238 **tissues**
239 The biological effect of NS1 and MMP-9 in the regulation of endothelial cell permeability was
240 evaluated. Firstly, the role of MMP-9 in the induction of endothelial cell permeability was
241 determined. HUVECs grown on polycarbonate membrane system were incubated with the
242 supernatants of DENV2-infected HUVEC cells or DENV2-infected THP-1 differentiated
243 macrophages or pre-incubated with SB-3CT (a specific inhibitor of MMP-9). Endothelial
244 permeability was evaluated by measuring trans-endothelial electrical resistance (TEER) (ohm) using
245 EVOM2 epithelial volt ohm meter. The level of TEER was not affected by the supernatants of
246 DENV-infected HUVECs; significantly attenuated by the supernatants of DENV-infected THP-1
247 differentiated macrophages from 3 h to 15 h post-treatment; and however, such reduction was
248 recovered by the treatment of SB-3CT (Fig 5A); suggesting that MMP-9 plays an important role in
249 the induction of endothelial hyperpermeability mediated by DENV infection. Next, we further
250 determined whether MMP-9 plays an important role in the induction of vascular permeability in mice
251 after DENV infection. *IFNAR*$^{-/-}$ C57BL/6 mice were treated with PBS as a control group (n = 4),
252 infected with DENV2 (n = 6), and intravenously treated with MMP-9 specific inhibitor SB-3CT and
253 then infected with DENV2(NGC) (n = 6). DENV2 E and NS5 RNA were detected at high levels in

the blood of DENV2-infected mice or SB-3CT-treated and DENV2-infected mice at 2 days and 4 days post-infection, but not detected in the blood of mocked-infected mice indicating that DENV2 replicated well in the mice (S2A and B Fig). It is worth noting that MMP-9 protein was significantly induced in the blood of DENV-infected mice, but not induced in the blood of mock-infected mice or SB-3CT-treated and DENV-infected both at 2 days, 4 days and 6 days post-treatment (Fig 5B, bottom); *MMP9* mRNA was significantly induced in the blood of DENV-infected or SB-3CT-treated and DENV-infected, but not induced in the blood of mock-infected mice at 2 days and 4 days post-treatment (Fig 5B, top). Moreover, the intensities of Evans blue dye in the Liver, Spleen and Lung of DENV-infected mice was significantly higher than that mock-infected mice or SB-3CT-treated and DENV-infected mice tissues (Fig 5C–E), suggesting that DENV infection induces vascular leakage in mice through promoting MMP-9 production. Meanwhile, Histopathology analysis showed that tissue injury like the spaces between the cells of tissue became larger in the Liver and Lung, the boundary between red pulp and white pulp were disrupted and the lymphatic nodules and pulping cells were increased in spleen were induced in DENV-infected mice organs compared with mock-infected mice tissues, but this phenomenon was rescued in SB-3CT-treated and DENV-infected mice tissues (Fig 5F–H). Additionally, HUVECs grown on Transwell inserts were incubated with purified MMP-9 protein, NS1 protein, and NS1 protein plus MMP-9 protein at different concentrations, or pre-treated with SB-3CT and then incubated with NS1 protein plus MMP-9 protein. The level of TEER was reduced by MMP-9 protein alone, NS1 protein alone, and MMP-9 protein plus NS1 protein from 2 to 7 h post-treatment; but the reductions were recovered by SB-3CT (Fig 5I); demonstrating that MMP-9 induces endothelial hyperpermeability in human endothelial cells.

276 **NS1 recruits MMP-9 to disrupts the junctions between endothelial cells**

277 Changes in endothelial cell permeability can be achieved by destroying the endothelial
278 glycocalyx layer (EGL) on the surface of endothelial cells or by altering the adhesion and tight
279 junctions between endothelial cells [12, 13]. Previous study reported that DENV NS1 disrupts the
280 EGL, leading to hyperpermeability [23]. However, the roles of NS1 in the regulation of the adhesion
281 and tight junctions between endothelial cells have not been reported. Here, the expression of junction
282 molecular include E-cadherin, ZO-2, α-E-catenin, and β-catenin was detected. The results showed
283 that E-cadherin, β-catenin, and ZO-2 proteins were down-regulated by DENV infection compared
284 with mock-infected mice in the liver (Fig 6A), spleen (Fig 6B), and lung (Fig 6C), but rescued in SB-
285 3CT-treated and DENV-infected mice (Fig 6A–C). Similarly, immunohistochemistry analyses also
286 showed that β-catenin was attenuated by DENV infection compared with mock-infected mice in the
287 liver (Fig 6D), spleen (Fig 6E), and lung (Fig 6F), but rescued in SB-3CT-treated and DENV-
288 infected mice (Fig 6D–F). Taken together, our results showed that DENV2 induces vascular leakage
289 through promoting MMP-9 to alter the adhesion and tight junctions in mice tissues.

290 Next, the effects of NS1 and MMP-9 on the regulation of adhesion and tight junction proteins
291 were determined. The adhesion junction proteins such as N-cadherin and β-catenin, and the tight
292 junction factors including Claudin-1 and Zona Occludens proteins (ZO-1, ZO-2, and ZO-3, also
293 known as tight junction proteins, TJP-1, TJP-2, and TJP-3) were not affected by NS1 in Hela cells
294 (S3A Fig) or HUVECs (Fig 6G). In contrast, the tight junction protein ZO-1, ZO-2 and the adhesion
295 junction protein β-catenin, N-cadherin were reduced by MMP-9, and such reductions were
296 eliminated by SB-3CT in both Hela (S3A Fig) and HUVEC cells (Fig 6G). Next, the levels of
297 endogenous β-catenin and ZO-1 proteins were visually evaluated by Immunofluorescence assays.

298 Hela cells and HUVECs were incubated with commercialized DENV2 NS1 protein or recombinant
299 human MMP-9 protein or NS1 protein plus MMP-9 protein. The levels of endogenous β-catenin
300 (S3B Fig and Fig 6H) and endogenous ZO-1 (S3C Fig and Fig 6I) were significantly reduced by NS1
301 protein and MMP-9 protein, and such reductions were recovered by SB-3CT in Hela cells (S3B and
302 C Fig) and HUVECs (Fig 6H and I).
303
304 **NS1 recruits MMP-9 to interact with adhesion and tight junction proteins**
305 The mechanism by which NS1 and MMP-9 induce endothelial hyperpermeability and vascular
306 leakage was evaluated. The interactions of NS1 and MMP-9 with adhesion and tight junction
307 proteins were determined. Co-IP results showed that NS1 and β-catenin interacted with each other in
308 both HEK293T cells and Hela cells (Fig 7A and B), but MMP-9 and β-catenin failed to interaction
309 with each other in HEK293T cells or Hela cells (S4A and B Fig). Similarly, NS1 and ZO-1
310 interacted with each other in both HEK293T cells and Hela cells (Fig 7C and D), while MMP-9 and
311 ZO-1 failed to interaction with each other in HEK293T cells or Hela cells (S4C and D Fig). These
312 results indicate that NS1 can interact with β-catenin and ZO-1, but MMP-9 cannot interact with β-
313 catenin and ZO-1. Interestingly, in Hela cells in the presence of NS1, MMP-9 and β-catenin
314 interacted with each other (Fig 7E and F), and similarly MMP-9 and ZO-1 also interacted with each
315 other (Fig 7G and H), indicating that NS1 facilitates MMP-9 to interacting with β-catenin or ZO-1.
316 Therefore, the results reveal that NS1 promotes MMP-9 to interact with adhesion and tight junction
317 proteins.
318
319 **NS1 induce vascular leakage through recruiting MMP-9 in mice**

320 Finally, the effects of NS1 and MMP-9 on the induction of vascular leakage were determined in
321 wild-type (C57BL/6) and MMP-9 deficient (MMP-$9^{-/-}$) mice. First, the knockout of the MMP-9 gene
322 was confirmed by genotyping using mouse tail DNA samples (S5 Fig). Next, C57BL/6 mice (n = 6,
323 six-week-old) and MMP-$9^{-/-}$ mice (n = 6, six-week-old) were injected (iv) with DENV2 NS1 protein
324 and/or recombinant mouse MMP-9 protein, followed by intravenous injection with Evans blue dye.
325 At 24 h post-treatment, the mice were euthanized, and mouse tissues were collected. Strikingly, the
326 intensities of Evans blue dye were enhanced by NS1 protein in the lung (Fig 8A), spleen (Fig 8B),
327 and liver (Fig 8C) of C57BL/6 mice. However, the intensities of Evans blue dye were relatively
328 unchanged by NS1 in the tissues of MMP-$9^{-/-}$ mice (Fig 8A–C). Interestingly, the intensities of Evans
329 blue dye were significantly enhanced by NS1 in the tissues of MMP-$9^{-/-}$ mice treated with MMP-9
330 (Fig 8A–C). Therefore, the results reveal that DENV NS1 induces vascular leakage in mouse tissues,
331 and demonstrate that MMP-9 is required for NS1-induced vascular leakages in mice. Moreover, the
332 effects of NS1 and MMP-9 on the production of adhesion and tight junction proteins in mice were
333 also determined. C57BL/6 mice (n = 6, six-week-old) and MMP-$9^{-/-}$ mice (n = 6, six-week-old) were
334 intravenously (via tail vein) injected with DENV2 NS1 protein and/or recombinant mouse MMP-9
335 protein. At 24 h post-treatment, the mice were euthanized, and mouse tissues were collected. β-
336 catenin and ZO-2 proteins were down-regulated by NS1 in the lung (Fig 8D), spleen (Fig 8E), and
337 liver (Fig 8F) of C57BL/6 mice, relatively unaffected by NS1 in MMP$9^{-/-}$ mouse tissues, and
338 significantly reduced by NS1 in the tissues of MMP$9^{-/-}$ mice treated with MMP-9 protein (Fig 8D–F).
339 Similarly, immunohistochemistry staining showed that β-catenin reduced by NS1 in the lung (Fig
340 8G), spleen (Fig 8H), and lives (Fig 8I) of C57BL/6 mice, relatively unaffected by NS1 in the tissues
341 of MMP$9^{-/-}$ mice, and significantly reduced by NS1 in the tissues of MMP$9^{-/-}$ mice treated with

342 MMP-9 protein (Fig 8G–I). Taken together, our findings demonstrate that NS1 induced endothelial
343 hyperpermeability in HUVECs and vascular leakages in mice, and revealed that MMP-9 is required
344 for NS1-induced endothelial hyperpermeability and vascular leakage (Fig 9).

346 **Discussion**

347

348 DENV infection may cause life-threatening diseases such as DHF, DSS, and ADE [28, 29]. The
349 clinical symptoms of DENV infection include hypotension, reduced blood volume, and vascular
350 permeability changes [30]. Therefore, it is important to investigate the mechanism by which DENV
351 infection increases vascular permeability. The present study revealed a distinct mechanism by which
352 DENV induces endothelial permeability and vascular leakage in human endothelial cells and mice
353 tissues.

354 Our initial results show that DENV2 promotes MMP-9 expression and secretion in human
355 PBMCs and macrophages. These results are consistent with previous reports that MMP-9 protein is
356 highly expressed in immune cells [15], but expressed at a very low level in endothelial cells [22].
357 More significantly, our findings demonstrate that DENV NS1 enhanced MMP-9 expression through
358 the activation of the NF-κB signaling pathway. Previous studies revealed that the surface of the
359 endothelial cells (ECs) is coated with a glycocalyx of membrane-bound macromolecules comprised
360 of sulfated proteoglycans, glycoproteins, and plasma proteins that adhere to the surface matrix [12],
361 MMP-9 is destructive to the integrity of endothelial cells and specifically degrades extracellular
362 matrix [14, 16], and DENV induces vascular leakage by up-regulating the expression of MMP-9 in
363 Dendritic cells (DCs) [17]. Here, we further demonstrate that NS1 interacts with the Zinc-binding
364 catalytic domain and the Fibronectin type-like domain of MMP-9 and facilitate the enzyme to alter
365 the adhesion and tight junctions, and thereby promoting vascular leakage, in human endothelial cells
366 and mice tissues including liver, spleen, and lung.

367 The maintenance of endothelial cell permeability is determined by two factors: (1) EGLs form

368 protective membranes on the surfaces of endothelial cells [11, 12], and (2) the adhesion and tight
369 junctions between endothelial cells maintain the integrity of endothelial cells [13]. It was reported
370 that NS1 induces vascular endothelial cell permeability leading to vascular leakage by disrupting the
371 extracellular polysaccharide-protein complexes [19, 20, 24], and NS1 acts as a pathogen-associated
372 molecular pattern (PAMP) by activating the Toll-like receptor 4 (TLR4) signaling pathways to
373 promote the release of inflammatory factors IL-6 and IL-8 and induce vascular leakage [20]. Recent
374 studies have further confirmed that macrophage migration inhibitory factor (MIF) plays a key role in
375 regulating NS1-induced degradation of extracellular polysaccharide proteins [22].

376 Interestingly, here we demonstrate that NS1 induces endothelial hyperpermeability in human
377 endothelial cells and mice tissues through activating MMP-9. The level of TEER are reduced by
378 MMP-9 and NS1, but the reductions are recovered by the specific inhibitor of MMP-9 (SB-3CT),
379 demonstrating that MMP-9 induces endothelial hyperpermeability in human endothelial cells.
380 Additionally, the intensities of Evans blue dye are enhanced by NS1 in the tissues of C57BL/6 mice;
381 relatively unaffected by NS1 in the tissues of MMP-9$^{-/-}$ mice; and significantly facilitated by NS1 in
382 the tissues of MMP-9$^{-/-}$ mice treated with MMP-9 protein; revealing that NS1 induces vascular
383 leakage in mice tissues, and demonstrating that MMP-9 is required for NS1-induced
384 hyperpermeability in mice tissues.

385 More interestingly, the mechanism by which NS1 and MMP-9 induce endothelial
386 hyperpermeability and vascular leakage is further revealed. The adhesion junction proteins N-
387 cadherin and β-catenin as well as the tight junction factors ZO-1, ZO-2, and ZO-3 are not affected by
388 NS1, but ZO-1, ZO-2, N-cadherin, and β-catenin are reduced by MMP-9, and such reductions are
389 eliminated by SB-3CT. Similarly, the endogenous ZO-1, ZO-2, N-cadherin, and β-catenin are

reduced by NS1 and MMP-9, and such reductions are recovered by SB-3CT. Additionally, β-catenin and ZO-2 are down-regulated by NS1 in of WT C57BL/6 mice tissues, relatively unaffected by NS1 in t MMP9$^{-/-}$ mice tissues, while significantly repressed by NS1 in the tissues of MMP9$^{-/-}$ mice supplemented with MMP-9 protein. Moreover, we further reveal that NS1 can interact with β-catenin and ZO-1; MMP-9 fails to interact with β-catenin and ZO-1; however, in the presence of NS1, MMP-9 associates with β-catenin and ZO-1; indicating that NS1 facilitates MMP-9 to interacting with β-catenin or ZO-1; and thereby degrading the adhesion and tight junction proteins. Taken together, these results demonstrate that NS1 induces hyperpermeability and vascular leakages in endothelial cells and mice tissues, and reveal that MMP-9 is required for NS1-induced endothelial hyperpermeability and vascular leakage through degrade ting the adhesion and tight junction proteins.

In summary, we reveal a distinct molecular mechanism by which the viral NS1 protein coordinates with the host factor MMP-9 to induce endothelial hyperpermeability and vascular leakage in human endothelial cells and mice tissues through disrupting the adhesion and tight junctions between endothelial cells. This study would provide new in signs into the pathogenesis caused by DENV infection, and suggest that MMP-9 may acts as a drug target for the prevention and treatment of DENV-associated diseases.

Materials and Methods

Clinical sample analysis

In this study, severe dengue patient samples were collected at Eight people's Hospital of Guangzhou during a DENV outbreak in Guangzhou, China, in 2014. Patients were categorized as having severe dengue according to the 2009 WHO criteria for dengue severity. All the dengue patient samples were assessed by anti-dengue IgM and IgG enzyme-linked immunosorbent assay (ELSIA) and qRT-PCR to quantify the DENV viral load. Serum samples from 8 patients with severe dengue were collected for ELISA analysis on day 2, day 5, day 8 and day 11 after hospitalization. In addition, 8 serum samples from healthy donors were include as the negative control. Informed consent was obtained from each person.

Animal studies

Wide-type (WT) C57BL/6 mice were purchased from Hubei Research Center of Laboratory Animals (Wuhan, Hubei, China). MMP9$^{-/-}$ mice were purchased from Model Animal Research Center of Nanjing University. *IFNAR*$^{-/-}$ C57BL/6 mice were bred in our laboratory. All mice were bred and maintained under specific pathogen-free conditions at Jinan University. For DENV2 infection assays, 6-week-old *IFNAR*$^{-/-}$ C57BL/6 mice were tail vein injected with PBS (mock infection), pre-treated with 300 μl PBS containing MMP-9 specific inhibitor SB-3CT (5 mg/kg per mice) by intraperitoneal injection for 90 min and then treated with DENV2 (1×10^6 PFU/mouse), repeat treated with SB-3CT (5 mg/kg per mice) on the fourth day after DENV2 (NGC) infection, or 300 μl PBS containing the same volume DMSO as a control group. One week after the DENV2

injection, mice were sacrificed, and tissues were collected for immunohistochemical and histopathological analyses. For other animal assays, six-week-old and sex-matched of MMP9$^{-/-}$ mice and Wide-type C57 BL/6 mice were randomly chosen to injection with DENV2-NS1 protein or recombinant mouse MMP-9 protein or DENV2-NS1 protein plus MMP-9 protein. The equivalent volumes of PBS-injected mice were used as negative controls. At 24 h post-injection, mice were sacrificed, and tissue were collected for Histopathology analysis.

Ethics statement.

All human subjects were adult. The study was conducted according to the principles of the Declaration of Helsinki and approved by the Institutional Review Board of the College of Life Sciences, Wuhan University in accordance with its guidelines for the protection of human subjects. The Institutional Review Board of the College of Life Sciences, Wuhan University, approved the collection of blood samples for this study, and it was conducted in accordance with the guidelines for the protection of human subjects. Written informed consent was obtained from each participant.

All animal studies were performed in accordance with the principles described by the Animal Welfare Act and the National Institutes of Health Guidelines for the care and use of laboratory animals in biomedical research. All procedures involving mice and experimental protocols were approved by the Institutional Animal Care and Use Committee (IACUC) of the College of Life Sciences, Wuhan University (Permit numbers: WDSKY0201901).

Cell culture

Human umbilical vein endothelial cells (HUCEV) were purchased form Obio Technology

(Shanghai, China). Human monocytic cell lines (THP-1), human embryonic kidney cell lines (HEK-293T), Hela cells, African green monkey cell lines (Vero) and Aedes albopictus gut cell lines (C6/36) were purchased from the American Type culture Collection (ATCC). THP-1 was grown in RPMI 1640 medium supplemented with 10% fetal calf serum, 100 U/ml penicillin, and 100 μg/ml streptomycin sulphate. HEK-293T, HUVEC and Vero were grown in DMEM medium with 10% fetal calf serum, 100 U/ml penicillin, and 100 μg/ml streptomycin sulphate. C6/36 was grown in MEM medium supplemented with 10% fetal calf serum, 100 U/ml penicillin, and 100 μg/ml streptomycin sulphate. THP-1, HEK-293T, HUVEC and Vero cells were maintained at 37°C in a 5% CO_2 incubator. C6/36 were maintained at 30°C in a 5% CO_2 incubator. In order to differentiation of macrophages. THP-1 were stimulated with Phorbol-12-myristate-13-acetate (PMA) for 12 h. Afterwards, cells were incubated for 24 h without PMA.

Peripheral blood mononuclear cells (PBMCs) were separated by density centrifugation of fresh peripheral venous blood samples that they were diluted 1:1 in pyrogen-free PBS over Histopaque (Haoyang Biotech). Then the cells were washed twice with PBS and resuspended in medium (RPMI 1640) supplemented with 10% FBS, penicillin (100 U/ml), streptomycin (100 μg/ml) in 6 well plates and 12 well plates.

Virus

All experiments used DENV-2 strain NGC (GenBank accession number KM204118.1) was kindly provided by Dr. Xulin Chen of Wuhan Institute of Virology, Chinese Academy of Sciences. To generate large stocks of dengue virus for experiments. C6/36 cells or Vero cells were incubated with DENV-2 at MOI of 0.5 for 2 h, then unbound dengue virus was washed away. The infected

474 cells were cultured sequentially in fresh medium with 2% FBS until seven days. Supernatants were
475 harvested and centrifuged at 4000 rpm for 10 min to remove cellular debris; then they were filtrated
476 by 0.22 μm filter membrane. All dengue virus was aliquoted into tubes for freezing at -70°C. Virus
477 tiles were determined by plaque assay using Vero cells.
478
479 **Regents and antibodies**
480 Phorbol-12-myristate-13-acetate (PMA), gelatin, Triton X-100, Coomassie brilliant blue R-250
481 was purchased from Sigma-Aldrich, MMP-9 inhibitor (SB-3CT) and NF-κB inhibitor (sc-75741)
482 were purchased from Selleck. Recombinant human MMP-9 protein and Recombinant mice MMP-9
483 protein were purchased from R&D systems. Commercialized DENV2-NS1 protein were purchased
484 from Native Antigen. Trizol reagent was purchased from Ambion. Lipofectamine 2000 reagent was
485 purchased from Invitrogen. Human MMP-9 ELISA kit was purchased from BD Biosciences. NF-κB
486 Pathway Sampler Kit (#9936T), Tight Junction Antibody Sampler Kit (#8683T), Cadherin-Catenin
487 Antibody Sampler Kit (#9961T) were purchased from Cell Signaling Technology. Antibody against
488 DENV-NS3 (GTX124252) were purchased from Genetex. Antibodies against Flag (F3165) and HA
489 (H6908) were purchased from Sigma. Anti-β-actin antibody (66009) were purchased from
490 Proteintech. Rabbit IgG and Mouse IgG were purchased from Invitrogen. Anti-Mouse IgG Dylight
491 649, Anti-Mouse IgG Dylight 488, Anti-Rabbit IgG Dylight 649, and Anti-Rabbit IgG FITC were
492 purchased from Abbkine.
493
494 **RNA extract and Real-time PCR**
495 Trizol reagent (Invitrogen, Carlsbad, CA) was used for total cellular RNA extracted according

to the manufacturer's instructions. Then the RNA (1 μg) were reverse transcribed to cDNA with 0.5 μl oligo (dT) and 0.5 μl Random primer at 37°C for 60 min and 72°C for 10 min. The cDNA then was used as templates for real-time PCR analysis. Real-time PCR was performed in a LightCycler 480 thermal cycler (Roche) by the following procedure: heat activate polymerase at 95°C for 5 min, afterwards, 45 cycles of 95°C for 15s, 58°C for 15s and 72°C for the 30s, the fluorescence was collected and analyzed at the 72°C step. A final melting curve step from 50°C to 95°C was used to test the specificity of the primer. The primers used in real-time PCR detection were listed in S1 Table.

Plasmids construction

Plasmid pcDNA3.1(+)-3×flag-Cap /prm /M /E /NS1 /NS2A /NS2B /NS3 /NS4A /NS4B /NS5 /MMP-9, Plasmid pCAggs-HA-MMP-9 /NS1 were constructed previously by our laboratory. The coding regions of β-catenin and ZO-1 were generated by PCR amplification. For β-catenin, the PCR production was inserted into the BamHI and XbaI sites of Plasmid pcDNA3.1(+)-3×flag. For ZO-1, the PCR production was inserted into the KpnI and EcoRV sites of Plasmid pcDNA3.1(+)-3×flag. For the truncated forms of MMP-9, the PCR productions were inserted into the EcoRI and XhoI sites of Plasmid pcDNA3.1(+)-3×flag. The sequences of primers were shown in S2 Table.

Zymography assay

MMP-9 proteinase activity was detected by the gelatin zymography assay as described previously. Briefly, the cells supernatants were separated in SDS-PAGE gels containing 1mg/ml gelatin. Then the gel was washed 3 times with 2.5% Triton X-100 (45 min every time), followed the

518 gel was washed with 50 mM Tris-HCl (pH7.6) containing 5 mM $CaCl_2$, 1 μM $ZnCl_2$ and 0.02%
519 sodium azide for 30 min. Afterwards, the gel was incubated overnight at 37°C in the same buffer,
520 then the gel was stained with 0.25% Coomassie brilliant blue R-250 for 2 h and then distaining.
521
522 **Enzyme-linked immunosorbent assay**
523 The concentration of culture supernatants and MMP-9 were measured by Human MMP-9
524 ELISA Kit (Invitrogen) according to manufacturer's instructions.
525
526 **Western-blot**
527 The PMA-differentiated THP-1 cells were collected and then washed twice with PBS and
528 dissolved in THP-1 lyses buffer (50 mM Tris-HCl, 150 mM NaCl, 0.1% Nonidetp40, 5 mM EDTA,
529 and 10% glycerol, pH7.4). The HEK-293T cells, HUVEC cells and Hela cells were prepared in 293T
530 lyses buffer (50 mM Tris-HCl, 300 mM NaCl, 1% Triton X-100, 5 mM EDTA, and 10% glycerol,
531 pH7.4). 10% protease inhibitor (Roche) were added to lyses buffer before using. Protein
532 concentration was measured by the Bradford assay (Bio-Rad, Richmond, CA). Cultured cell lysates
533 (50 μg) were electrophoresed in an 8–12% SDS polyacrylamide gels and transferred to nitrocellulose
534 membranes (Amersham, Piscataway, NJ). Nonspecific bands of NC membranes were blocked by
535 using 5% skim milk for 2 h. Then membranes were washed third with phosphate buffered saline with
536 0.1% Tween 20 (PBST) and incubated with the specific antibody. Protein bands were visualized
537 using a Luminescent Image Analyzer (Fujifilm LAS-4000).
538
539 **Co-immunoprecipitation assays**

HEK-293T cells or Hela cells were spread to 6-cm-diameter dishes, and co-transfected with the purpose of plasmids for 24 h. Then the cells were lysed in 293T lyses buffer (50 mM Tris-HCl, 300 mM NaCl, 1% Triton X-100, 5 mM EDTA, and 10% glycerol, pH7.4), The lyses buffer was rotating at 4°C for 30 min and centrifuged at 12000 rpm for 15 min to remove cellular debris. A little part of supernatants was sucked out as Input, and the others were incubated with the indicated antibodies overnight at 4°C.Then mixed with the Protein G sepharose beads (GE Healthcare) for 2 h at 4°C.The immunoprecipitates were washed four to six times with the 293T lyses buffer (50 mM Tris-HCl, 300 mM NaCl, 1% Triton X-100, 5 mM EDTA, and 10% glycerol, pH7.4), boiled in protein loading buffer for 10 min. Then analyzed by using SDS-PAGE and Western blotting.

Immunofluorescence

HEK-293T cells were grown on sterile cover slips were transfected with HA-MMP-9 and Flag-NS1 at 40% confluence for 24 h. HUVEC cells or Hela cells were grown on sterile cover slips at 80% confluence, then treated with NS1 protein (5 μg/ml) or MMP-9 protein (100 ng/ml) or NS1 (5 μg/ml) plus MMP-9 (100 ng/ml) or pre-incubated with 600 nM SB-3CT for 1h, then treated with NS1 (5 μg/ml) plus MMP-9 (100 ng/ml) for 6 h. Cells were fixed with 4% paraformaldehyde for 15 min and then washed three times with wash buffer (ice-cold PBS containing 0.1% BSA), permeabilized with PBS containing 0.2% TritonX-100 for 5 min and washed three times with wash buffer, after blocking with 5% BSA for 30 min, cells were incubated overnight with anti-HA antibody and anti-Flag antibody (1:200 in wash buffer) or anti-β-catenin or anti-ZO-1 antibody (1:100 in wash buffer), followed by staining with FITC-conjugated donkey anti-mouse IgG and Daylight 649-conjugated donkey anti-rabbit IgG or just Cy3-conjugated donkey anti-mouse IgG

562 secondary antibody (Abbkine) (1:100 in wash buffer) for 1 h. Nuclei were stained with DAPI for 5
563 min, and then the cells were washed three times with wash buffer. Finally, the cells were viewed
564 using a confocal fluorescence microscope (Fluo View FV1000; Olympus, Tokyo, Japan).
565
566 **Quantization of vascular leakage in vivo**
567 The level of vascular leakage in mice was quantified through Evans blue assays as previously
568 described. Briefly, 300 μl of 0.5% Evans blue dye was injected intravenously to five groups and
569 allowed the dye to circulate for 2 h. Then the mice were euthanized and extensively perfused with
570 PBS. Tissues was collected and weighed. The tubes containing tissue were added to 1 ml formamide
571 and incubated at 37°C for 24 h. Evans blue concentration was quantified by measuring OD_{610} and
572 comparing to the standard curve. Data was expressed as ng Evans blue dye/ mg tissue weight.
573
574 **Trans-endothelial electrical resistance (TEER)**
575 Human umbilical vein endothelial cells (HUVEC) monolayers were grown on the 24-well
576 transwell polycarbonate membrane system (Transwell permeable support, 0.4 m, 6.5 mm insert;
577 Corning Inc.), and then treated with different reagents. After 24 h of treatment, 50% of upper and
578 lower chamber media was replaced by fresh endothelial cell medium. Untreated endothelial cells
579 grown on Transwell inserts were used as negative controls and medium alone were used for blank
580 controls. Endothelial permeability was evaluated by measuring TEER in ohms at indicated time
581 points using EVOM2 epithelial voltohmmeter (World Precision Instruments). Relative TEER was
582 expressed as follows: [ohm (experimental groups) - ohm (medium alone)] / [ohm (untreated
583 endothelial cells) - ohm (medium alone).

584

585 **Statistical analysis**

586 All experiments were repeated two to three times with similar results. All results were
587 expressed as the mean ± the standard deviation (SD). Statistical analysis was carried out using the t-
588 test for two groups and one-way ANOVA for multiple groups (GraphPad Prism5). The date was
589 considered statistically significant when $P \leq 0.05$ (*), $P \leq 0.01$ (**), $P \leq 0.001$ (***).

Acknowledgments

We thank Dr. Jincun Zhao of the First Affiliated Hospital of Guangzhou Medical University, Guangzhou, China, for the gift of IFNAR$^{-/-}$C57BL/6 mice deficient in IFN-α/β receptors, Dr. Xulin Chen of Wuhan Institute of Virology, Chinese Academy of Sciences, for the gift of DENV-2 strain NGC (GenBank accession number KM204118.1).

597 **References**

598

599 1. Bhatt S, Gething PW, Brady OJ, Messina JP, Farlow AW, Moyes CL, et al. The global
600 distribution and burden of dengue. Nature 2013; 496(7446):504-7.
601 2. Swaminathan S, Khanna N. Dengue: recent advances in biology and current status of
602 translational research. Curr Mol Med 2009; 9(2):152-73.
603 3. Guha-Sapir D, Schimmer B. Dengue fever: new paradigms for a changing epidemiology. Emerg
604 Themes Epidemiol 2005; 2(1):1.
605 4. WHO. Ten threats to global health in 2019 [EB/OL]. https://www.who.int/news-room/feature-
606 stories/ten-threats-to-global-health-in-2019.
607 5. Pang T, Cardosa MJ, Guzman MG. Of cascades and perfect storms: the immunopathogenesis of
608 dengue haemorrhagic fever-dengue shock syndrome (DHF/DSS). Immunol Cell Biol 2007;
609 85(1):43-5.
610 6. Narvaez F, Gutierrez G, Pérez MA, Elizondo D, Nuñez A, Balmaseda A, et al. Evaluation of the
611 traditional and revised WHO classifications of Dengue disease severity. PLoS Negl Trop Dis
612 2011; 5(11):e1397.
613 7. Vervaeke P, Vermeire K, Liekens S. Endothelial dysfunction in dengue virus pathology. Rev
614 Med Virol 2015; 25(1):50-67.
615 8. Levy A, Valero N, Espina LM, Añez G, Arias J, Mosquera J. Increment of interleukin 6, tumour
616 necrosis factor alpha, nitric oxide, C-reactive protein and apoptosis in dengue. Trans R Soc Trop
617 Med Hyg 2010;104(1):16-23.
618 9. Pan P, Zhang Q, Liu W, Wang W, Yu Z, Lao Z, et al. Dengue virus infection activates

619 interleukin-1β to induce tissue injury and vascular leakage. Front Microbiol 2019; 10:2637.
620 10. Liu P, Woda M, Ennis FA, Libraty DH. Dengue virus infection differentially regulates
621 endothelial barrier function over time through type I interferon effects. J Infect Dis 2009;
622 200(2):191-201.
623 11. Weinbaum S, Tarbell JM, Damiano ER. The structure and function of the endothelial glycocalyx
624 layer. Annu Rev Biomed Eng 2007; 9:121-67.
625 12. Reitsma S, Slaaf DW, Vink H, van Zandvoort MA, oude Egbrink MG. The endothelial
626 glycocalyx: composition, functions, and visualization. Pflugers Arch 2007; 454(3):345-59.
627 13. Dejana E. Endothelial cell-cell junctions: happy together. Nat Rev Mol Cell Biol 2004; 5(4):261-
628 70.
629 14. Asahi M, Wang X, Mori T, Sumii T, Jung JC, Moskowitz MA, et al. Effects of matrix
630 metalloproteinase-9 gene knock-out on the proteolysis of blood-brain barrier and white matter
631 components after cerebral ischemia. J Neurosci 2001; 21(19):7724-32.
632 15. Björklund M, Koivunen E. Gelatinase-mediated migration and invasion of cancer cells. Biochim
633 Biophys Acta 2005; 1755(1):37-69.
634 16. Vandooren J, Van den Steen PE, Opdenakker G. Biochemistry and molecular biology of
635 gelatinase B or matrix metalloproteinase-9 (MMP-9): the next decade. Crit Rev Biochem Mol
636 Biol 2013; 48(3):222-72.
637 17. Luplertlop N, Missé D, Bray D, Deleuze V, Gonzalez JP, Leardkamolkarn V, et al. Dengue-
638 virus-infected dendritic cells trigger vascular leakage through metalloproteinase overproduction.
639 EMBO Rep 2006; 7(11):1176-81.
640 18. Van Teeffelen JW, Brands J, Stroes ES, Vink H. Endothelial glycocalyx: sweet shield of blood

641 vessels. Trends Cardiovasc Med 2007;17(3):101-5.

642 19. Beatty PR, Puerta-Guardo H, Killingbeck SS, Glasner DR, Hopkins K, Harris E. Dengue virus
643 NS1 triggers endothelial permeability and vascular leak that is prevented by NS1 vaccination.
644 Sci Transl Med 2015;7(304):304ra141.

645 20. Modhiran N, Watterson D, Muller DA, Panetta AK, Sester DP, Liu L, et al. Dengue virus NS1
646 protein activates cells via Toll-like receptor 4 and disrupts endothelial cell monolayer integrity.
647 Sci Transl Med 2015;7(304):304ra142.

648 21. Chen HR, Chuang YC, Lin YS, Liu HS, Liu CC, Perng GC, et al. Dengue Virus Nonstructural
649 Protein 1 Induces Vascular Leakage through Macrophage Migration Inhibitory Factor and
650 Autophagy. PLoS Negl Trop Dis 2016; 10(7):e0004828.

651 22. Chen HR, Chao CH, Liu CC, Ho TS, Tsai HP, Perng GC, et al. Macrophage migration inhibitory
652 factor is critical for dengue NS1-induced endothelial glycocalyx degradation and
653 hyperpermeability. PLoS Pathog 2018; 14(4):e1007033.

654 23. Puerta-Guardo H, Glasner DR, Harris E. Dengue virus NS1 disrupts the endothelial glycocalyx,
655 leading to hyperpermeability. PLoS Pathog 2016;12(7):e1005738.

656 24. Glasner DR, Ratnasiri K, Puerta-Guardo H, Espinosa DA, Beatty PR, Harris E. Dengue virus
657 NS1 cytokine-independent vascular leak is dependent on endothelial glycocalyx components.
658 PLoS Pathog 2017; 13(11):e1006673.

659 25. Gutsche I, Coulibaly F, Voss JE, Salmon J, d'Alayer J, Ermonval M, et al. Secreted dengue virus
660 nonstructural protein NS1 is an atypical barrel-shaped high-density lipoprotein. Proc Natl Acad
661 Sci U S A 2011;108(19):8003-8.

662 26. Opdenakker G, Van den Steen PE, Dubois B, Nelissen I, Van Coillie E, Masure S, et al.

663 Gelatinase B functions as regulator and effector in leukocyte biology. J Leukoc Biol
664 2001;69(6):851-9.
665 27. Marovich M, Grouard-Vogel G, Louder M, Eller M, Sun W, Wu SJ, et al. Human dendritic cells
666 as targets of dengue virus infection. J Investig Dermatol Symp Proc 2001;6(3):219-24.
667 28. Recker M, Blyuss KB, Simmons CP, Hien TT, Wills B, Farrar J, et al. Immunological serotype
668 interactions and their effect on the epidemiological pattern of dengue. Proc Biol Sci 2009;
669 276(1667):2541-8.
670 29. Katzelnick LC, Gresh L, Halloran ME, Mercado JC, Kuan G, Gordon A, et al. Antibody-
671 dependent enhancement of severe dengue disease in humans. Science 2017; 358(6365):929-32.
672 30. Yacoub S, Wertheim H, Simmons CP, Screaton G, Wills B. Microvascular and endothelial
673 function for risk prediction in dengue: an observational study. Lancet 2015; 385 Suppl 1:S102.
674

675 **Figure legends**

676

677 **Fig 1. DENV induces the production of NS1, MMP-9 and TIMP-1 in severe dengue patients.**

678 (**A**–**C**) The serum concentration of NS1(A), MMP-9 (B) and TIMP-1 (C) in healthy donors and

679 severe dengue patients infected days (2, 5, 8, and 11 days) was measured by ELISA. Points represent

680 the value in each serum sample.

681 (**D**–**F**) the correlations of the concentrations of NS1 and MMP-9 (D), TIMP-1 and MMP-9 (E) and

682 TIMP-1 and NS1 (F) in the same group of severe dengue patients infected 11 days were plotted.

683 Linear regressions were traced according to the distributions of the points.

684 Dates were representative of two independent experiments. $P \leq 0.05$ (*), $P \leq 0.01$ (**), $P \leq 0.001$

685 (***).

686

687 **Fig 2. DENV NS1 interacts with MMP-9.**

688 (**A**) HEK293T cells were co-transfected with *HA-MMP-9* and *Flag-Cap, Flag-M, Flag-Prm, Flag-E,*

689 *Flag-NS1, Flag-NS2A, Flag-NS2B, Flag-NS3, Flag-NS4A or Flag-NS4B*. Cell lysates were

690 immunoprecipitataed using anti-Flag antibody, and analyzed using anti-Flag and anti-HA antibody.

691 Cell lysates (40 μg) was used as Input.

692 (**B**) HEK293T cells were co-transfected with *HA-MMP9* and *Flag-NS1*, Cell lysates were

693 immunoprecipitataed using anti-HA antibody, and analyzed using anti-Flag and anti-HA antibody.

694 Cell lysates (40 μg) was used as Input.

695 (**C**) HEK293T cells were co-transfected with *Flag-N*C and *HA-MMP-9*, *Flag-N*S1 and *HA-NC,* or

696 *Flag-NS1* and *HA-MMP-9*, sub-cellular localization of *HA-MMP-9* and *Flag-NS1* and DAPI were

visualized under confocal microscope.

(**D**) Schematic diagram of wild-type MMP-9 protein and truncated mutants MMP-9 protein (D1 to D9). HEK293T cells were co-transfected with *HA-NS1* and *Flag-MMP-9* truncated mutants (D1-D9). Cell lysates were immunoprecipitataed using anti-Flag antibody, and analyzed using anti-Flag and anti-HA antibody. Cell lysates (40 μg) was used as Input.

Dates were representative of three independent experiments.

Fig 3. NS1 activates MMP-9 expression through the NF-κB signaling pathway.

(**A**) PMA-differentiated THP-1 macrophages were transfected with the different concentrations of plasmid encoding *NS1* for 24h. Cell lysates were analyzed (top) by immunoblotting. Supernatants were analyzed (middle) by gelatin zymography assays for MMP-9 proteinase activity. Intracellular *MMP-9* RNA (bottom) was determined by qRT-PCR analysis. TIMP-1 protein in cell supernatants were measured by ELISA

(**B**) HEK293T cells were co-transfected with the plasmid encoding *MMP-9* and different concentrations of plasmid encoding *NS1* for 24 h. Cell lysates were analyzed (top) by immunoblotting. Supernatants were analyzed (middle) by gelatin zymography assays for MMP-9 proteinase activity. Intracellular *MMP-9* RNA (bottom) was determined by qRT-PCR analysis.

(**C**) HEK293T cells were con-transfected with different concentrations of *NS1* expressing plasmid and *NF-κB* reporter plasmid. Luciferase assays were performed 20h after transfection.

(**D**) PMA-differentiated THP-1 macrophages were firstly transfected with plasmid encoding *HA-CT* or *HA-NS1* for 20 h, and then treated with 200 nM SC75741 for 5 h, MMP-9 protein in cell supernatants were measured by ELISA (top) and indicated proteins in cell extract were analyzed by

719 WB (middle). Intracellular *MMP-9* RNA (bottom) was determined by qRT-PCR analysis.

720 (**E**–**G**) PMA-differentiated THP-1 macrophages (E), Hela cells (F) and HEK293T cells (G) were

721 transfected with different concentrations of plasmid encoding *NS1* for 24h. The indicated proteins in

722 cell extract were analyzed by WB.

723 Dates were representative of two to three independent experiments. Values are mean ± SEM, $P \leq$

724 0.05 (*), $P \leq 0.01$ (**), $P \leq 0.001$ (***).

725

726 **Fig 4. DENV2 induces MMP-9 expression and secretion in human PBMCs and macrophages,**

727 **but not in HUVECs.**

728 (**A** and **B**) PMA-differentiated THP-1 macrophages were infected with DENV2 for different times at

729 MOI=5 (A) or at different MOI for 24 h (B). Intracellular *MMP-9* RNA (top) and DENV2 *E* RNA

730 (bottom) was determined by qRT-PCR analysis, MMP-9 proteinase activity in the supernatants was

731 determined by gelatin zymography assays and proteins in cell extract (middle) were analyzed by

732 Western blotting.

733 (**C** and **D**) HUVEC cells were infected with DENV2 for different times at MOI=5 (C) and at

734 different MOI for 24 h (D). Intracellular *MMP-9* RNA (top) and DENV2 *E* RNA (bottom) was

735 determined by qRT-PCR analysis, MMP-9 proteinase activity in the supernatants was determined by

736 gelatin zymography assays and proteins in cell extract (middle) were analyzed by Western blotting.

737 (**E**) HUVEC cells or PMA-differentiated THP-1 macrophages were infected with DENV2 at MOI =

738 5 for 24 h. The mRNA level of DENV2 *E* protein were measured by qRT-PCR.

739 (**F**) HUVEC cells or PMA-differentiated THP-1 macrophages were equally distributed to four 12-

740 hole plates for 24 h. MMP-9 protein in cell supernatants were measured by ELISA (top) and

741 indicated proteins in cell extract were analyzed by WB (bottom).

742 Dates were representative of three independent experiments. Values are mean ± SEM, P ≤0.05 (*), P

743 ≤0.01 (**), P ≤0.001 (***).

744

745 **Fig 5. NS1 facilitates MMP-9 to induce endothelial hyperpermeability in human cells and mice**

746 **tissues.**

747 (**A**) Confluent monolayers of HUVEC cells were grown on polycarbonate membrane system and

748 treated with the supernatants came from DENV2 infected HUVEC cells or THP-1 cells for 24 h or

749 pre-incubated with 600nM SB-3CT (a specific inhibitor of MMP-9 protein) for 1h. Endothelial

750 permeability was evaluated by measuring trans-endothelial electrical resistance (TEER) (ohm) using

751 EVOM2 epithelial voltohmmeter.

752 (**B**–**H**) *IFNAR*$^{-/-}$ C57BL/6 mice were intravenously injected with 300 μl DENV2 at a dose of 1×10^6

753 PFU/mouse (n = 6) , pre-treated with 300 μl PBS containing MMP-9 specific inhibitor SB-3CT (5

754 mg/kg per mice) by intraperitoneal injection for 90 min and then treated with DENV2 (1×10^6

755 PFU/mouse), repeat treated with SB-3CT (5 mg/kg per mice) on the fourth day after DENV2 (NGC)

756 infection (n = 6), or 300 μl PBS containing the same volume DMSO as a control group (n = 4). 7

757 days after infection, mice were euthanasia, and the tissues were collected. *MMP-9* RNA in the blood

758 was determined by qRT-PCR (upper) and MMP-9 protein in the serum was measured by ELISA

759 (lower). Points represent the value of each serum samples (B). Evans blue dye was intravenously

760 injected into mice 7 days after DENV infected groups (n = 5), control groups (n = 4) and

761 DENV+SB-3CT (n = 5) (C–E). The dye was allowed to circulate for 2 hours before mice were

762 euthanasia, tissues include liver (C), spleen (D) and lung (E) were collected, and the value of Evans

763 blue was measured at OD_{610}. Histopathology analysis of tissues includes Liver (F), Spleen (G) and
764 Lung (H) after DENV infection.
765 (**I**) Monolayers of HUVEC cells grown on Transwell inserts were incubated for 48 h with MMP-9
766 protein (100 ng/ml) or NS1 protein (5 μg/ml) or NS1 (5 μg/ml) plus different concentration of MMP-
767 9 (50 ng/ml to 100ng/ml) or pre-treated with 600 nM SB-3CT for 1 h, then incubated with NS1 plus
768 MMP-9. The TEER (ohm) was measured at indicated time points.
769 Dates were representative of two to three independent experiments. Values are mean ± SEM, $P \leq 0.05$
770 (*), $P \leq 0.01$ (**), $P \leq 0.001$ (***).
771
772 **Fig 6. NS1 recruits MMP-9 to disrupts the junctions between endothelial cells.**
773 (**A**–**F**) *IFNAR*$^{-/-}$ C57BL/6 mice were intravenously injected with 300 μl DENV2 at a dose of 1×10^6
774 PFU/mouse (n = 6) , pre-treated with 300 μl PBS containing MMP-9 specific inhibitor SB-3CT (5
775 mg/kg per mice) by intraperitoneal injection for 90 min and then treated with DENV2 (1×10^6
776 PFU/mouse), repeat treated with SB-3CT (5 mg/kg per mice) on the fourth day after DENV2 (NGC)
777 infection (n = 6), or 300 μl PBS containing the same volume DMSO as a control group (n = 4). 7
778 days after infection, mice were euthanasia, and the tissues were collected. The indicated proteins in
779 Lung (A), spleen (B) and Liver (C) were measured by Western-blot. The expression of β-catenin in
780 Liver (D), spleen (E), and Lung (F) by Immunohistochemistry analysis.
781 (**G**) HUVEC cells were respectively transfected with plasmid encoding *MMP-9* (2 μg) or *NS1* (2 μg)
782 or *NS1* (1 ug) plus *MMP-9* (1 μg) for 24 h or firstly co-transfected with plasmid encoding *NS1* (1ug)
783 plus *MMP-9* (1 μg) for 12 h, then treated with 600nM SB-3CT for 12 h. The indicated proteins in
784 cell extract were analyzed by WB.

(**H** and **I**) HUVEC cells were treated with NS1 protein (5 μg/ml) or MMP-9 protein (100 ng/ml) or NS1 (5 μg/ml) plus MMP-9 (100 ng/ml) or pre-incubated with 600 nM SB-3CT for 1 h, then treated with NS1 (5 μg/ml) plus MMP-9 (100 ng/ml) for 6 h, The distribution of endogenous β-catenin (H) or ZO-1 (I) protein were visualized under confocal microscope.

All dates were representative of two to three independent experiments.

Fig 7. NS1 recruits MMP-9 to interact with adhesion and tight junction proteins.

(**A**) HEK293T cells were transfected with plasmid encoding *HA-NS1* plus *Flag-β-catenin*. Cell lysates were immunoprecipitated using anti-Flag or anti-HA antibody, and analyzed using anti-Flag, anti-HA or anti-β-catenin antibody. Cell lysates (40 μg) was used as Input.

(**B**) Hela cells were transfected with plasmid encoding *HA-NS1*, Cell lysates were immunoprecipitated using anti-HA or anti-β-catenin antibody, and analyzed using anti-HA or anti-β-catenin antibody. Cell lysates (40 μg) was used as Input.

(**C** and **D**) HEK293T cells (C) or Hela cells (D) were co-transfected with plasmid encoding *HA-NS1* plus *Flag-ZO-1*, Cell lysates were immunoprecipitated using anti-Flag or anti-HA antibody, and analyzed using anti-Flag or anti-HA antibody. Cell lysates (40 μg) was used as Input.

(**E** and **F**) Hela cells were co-transfected with plasmid encoding *HA-NS1* plus *Flag-MMP-9*, Cell lysates were immunoprecipitated using anti-Flag (E) or anti-β-catenin antibody (F), and analyzed using anti-Flag, anti-HA or anti-β-catenin antibody. Cell lysates (40 μg) was used as Input.

(**G** and **H**) Hela cells were co-transfected with plasmid encoding *HA-NS1*, *HA-MMP-9* (G) and *Flag-ZO-1* or *Flag-NS1*, *HA-MMP-9* and *Flag-ZO-1* (H). Cell lysates were immunoprecipitated using anti-Flag (G) or anti-HA antibody (H), and analyzed using anti-Flag, anti-HA or anti-MMP-9

807 antibody. Cell lysates (40 μg) was used as Input.

808 All dates were representative of three independent experiments.

809

810 **Fig 8. NS1 induce vascular leakage through recruiting MMP-9 in mice.**

811 C57BL/6 mice and MMP-9$^{-/-}$ mice were injected intravenously DENV2 NS1 protein [10 mg/kg (n =

812 5)], the same volume of PBS was also tail vein injected to C57BL/6 mice and MMP-9$^{-/-}$- mice (n = 5)

813 as control group. Another group of MMP-9$^{-/-}$ mice (n = 5) were injected intravenously DENV2 NS1

814 protein (10 mg/kg) plus recombinant mouse MMP-9 protein (70 μg /kg).

815 (**A**–**C**) After 24 h post-injection, mice were intravenously injected with Evans blue dye. The dye was

816 allowed to circulate for 2h before mice were euthanized, and tissue include Lung (A), spleen (B) and

817 Liver (C) were collected. The value of Evans blue was measured at OD_{610}.

818 (**D**–**I**) After 24h post-injection, mice were euthanized and tissue were collected. The indicated

819 proteins in Lung (D), spleen (E), and Liver (F) were measured by Western-blot. The expression of β-

820 catenin in Lung (G), spleen (H), and Liver (I) were analyzed by Immunohistochemistry.

821 All dates were representative of two to three independent experiments. Values are mean ± SEM, P

822 ≤0.05 (*), P ≤0.01 (**), P ≤0.001 (***).

823

824 **Fig 9. A proposed model in which DENV NS1 and MMP-9 coordinate to induce vascular**

825 **leakage by altering endothelial cell adhesion and tight junctions.**

826 DENV non-structural protein 1 (NS1) induces MMP-9 expression through activating the nuclear

827 factor κB (NF-κB) signaling pathway. Additionally, NS1 interacts with MMP-9 and facilitates the

828 enzyme to alter the adhesion and tight junctions and vascular leakage in human endothelial cells and

829 mice tissues. Moreover, NS1 recruits MMP-9 to interact with β-catenin and Zona occludens protein-

830 1/2 to degrade the important adhesion and tight junction proteins, thereby inducing endothelial

831 hyperpermeability and vascular leakage in human endothelial cells and mice tissues.

Supporting information

S1 Fig. DENV2 induces MMP-9 expression and secretion in human PBMCs.

(**A** and **B**) Human PBMCs were infected with DENV2 for different times at MOI=5 (A) or at different concentrations for 24 h (B). Intracellular *MMP-9* RNA (top) and DENV2 *E* RNA (bottom) was determined by qRT-PCR analysis and MMP-9 proteinase activity in the supernatants was determined by gelatin zymography assays (middle).

Dates were representative of two to three independent experiments. Values are mean ± SEM, P ≤0.05 (*), P ≤0.01 (**), P ≤0.001 (***).

S2 Fig. Detection of DENV infection in mice.

(**A** and **B**) *IFNAR*$^{-/-}$ C57BL/6 mice were intravenously injected with 300 μl DENV2 at a dose of 1×10^6 PFU/mouse (n = 6) , pre-treated with 300 μl PBS containing MMP-9 specific inhibitor SB-3CT (5 mg/kg per mice) by intraperitoneal injection for 90 min and then treated with DENV2 (1×10^6 PFU/mouse), repeat treated with SB-3CT (5 mg/kg per mice) on the fourth day after DENV2 (NGC) infection (n = 6), or 300 μl PBS containing the same volume DMSO as a control group (n = 4). 7 days after infection, mice were euthanasia, and the tissues were collected. Blood samples were collected at 2, 4, and 6 days post-infection. DENV2 *E* (A) and *NS5* (B) RNA was determined by qRT-PCR. Points represent the value of each blood samples.

Dates were representative of two independent experiments. P ≤0.05 (*), P ≤0.01 (**), P ≤0.001 (***).

S3 Fig. NS1 through recruiting MMP-9 to Destroy the junctional molecules in Hela cells.

(**A**) Hela cells were respectively transfected with plasmid encoding *MMP-9* (2 μg) or *NS1* (2 μg) or *NS1* (1 ug) plus *MMP-9* (1 μg) for 24 h or firstly co-transfected with plasmid encoding *NS1* (1ug) plus *MMP-9* (1 μg) for 12 h, then treated with 600nM SB-3CT for 12 h. The indicated proteins in cell extract were analyzed by WB.

(**B** and **C**) Hela cells were treated with NS1 protein (5 μg/ml) or MMP-9 protein (100 ng/ml) or NS1 (5 μg/ml) plus MMP-9 (100 ng/ml) or pre-incubated with 600nM SB-3CT for 1 h, then treated with NS1 (5 μg/ml) plus MMP-9 (100 ng/ml) for 6 h, The distribution of endogenous β-catenin (B) or ZO-1 (C) protein were visualized under confocal microscope.

Dates were representative of three independent experiments.

S4 Fig. MMP-9 have no interaction with the junctional molecules.

(**A** and **B**) HEK293T cells (A) or Hela cells (B) were transfected with plasmid encoding *Flag-MMP-9*. Cell lysates were immunoprecipitated using anti-Flag or anti-β-catenin antibody, and analyzed using anti-Flag or anti-β-catenin antibody. Cell lysates (40 μg) was used as Input.

(**C** and **D**) HEK293T cells (C) or Hela cells (D) were transfected with plasmid encoding *HA-MMP-9* plus *Flag-ZO-1*, Cell lysates were immunoprecipitated using anti-HA or anti-Flag antibody, and analyzed using anti-Flag or anti-MMP-9 antibody. Cell lysates (40 μg) was used as Input.

All dates were representative of three independent experiments.

S5 Fig. Detection of MMP-9 knockout mice.

C57BL/6 mice and MMP-$9^{-/-}$ mice were injected intravenously DENV2 NS1 protein [10mg/kg (n =

876 5)], the same volume of PBS was also tail vein injected to C57BL/6 mice and MMP-9$^{-/-}$- mice (n = 5)
877 as control group. Another group of MMP-9$^{-/-}$ mice (n = 5) were injected intravenously DENV2 NS1
878 protein (10 mg/kg) plus recombinant mouse MMP-9 protein (70 μg/kg). After 24h post-injection.
879 The tails randomly selected from five groups (Four mice came from wild type C57BL/6 and twelve
880 mice came from MMP-9$^{-/-}$ mice), the total genome was extracted from the tail of mice. The knock-
881 out level of MMP-9 was detected by specific primers.

882

883 **Supporting Tables**

884

885 **S1 Table. qRT-PCR Primers used in this study.**

886

887 **S2 Table. Primers used for plasmids construction in this study.**

Figure 1

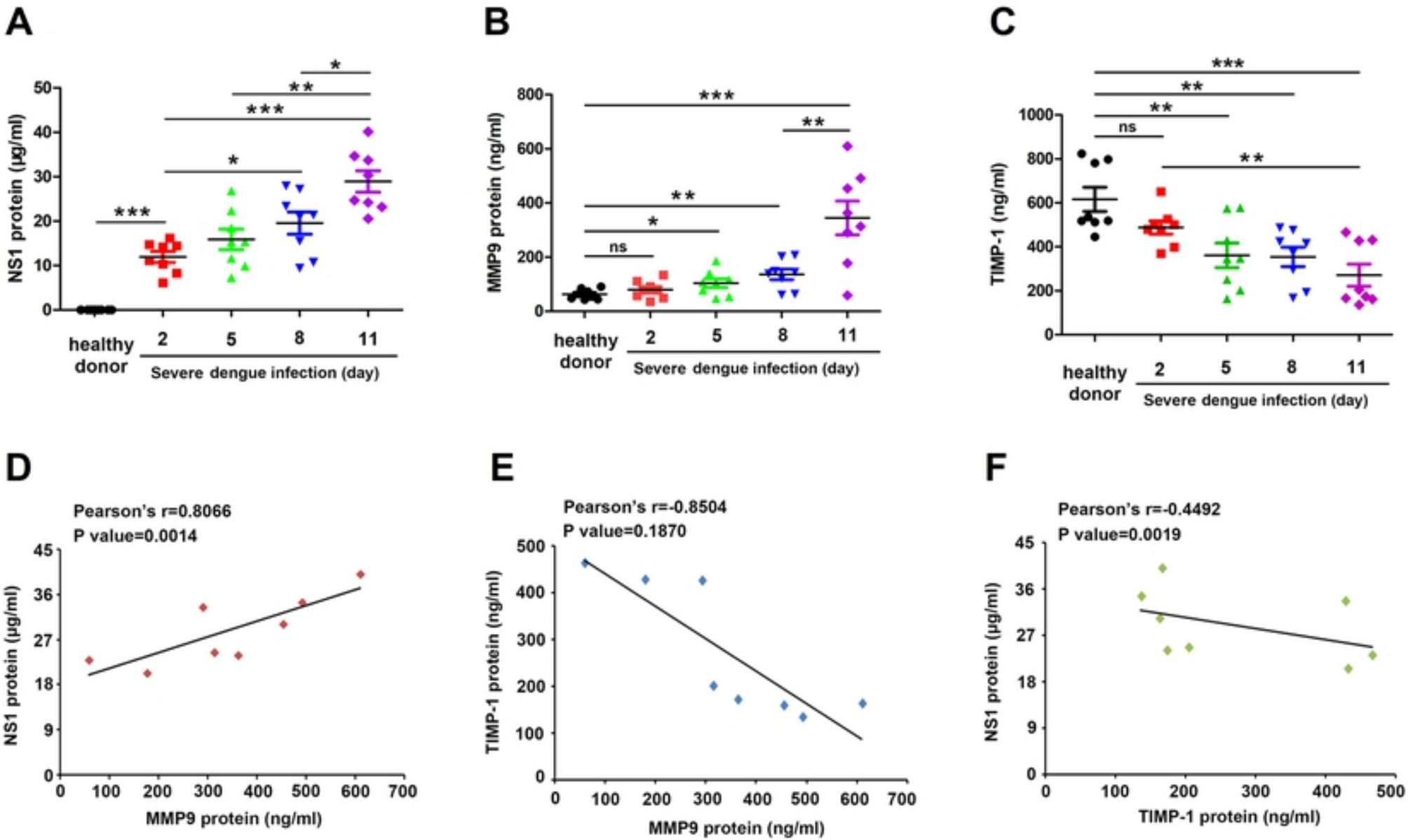

Figure 1

Figure 2

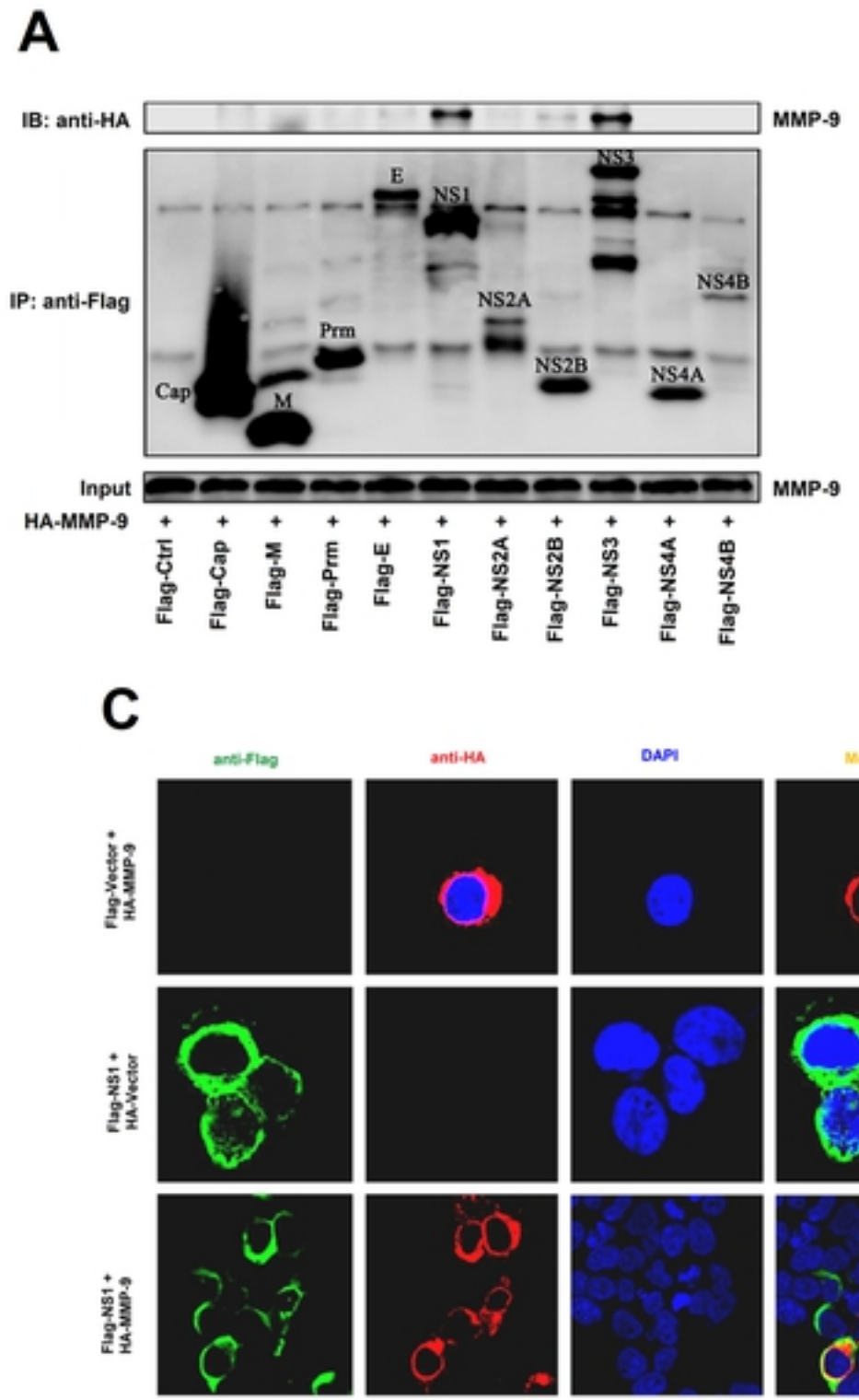

Figure 2

Figure 3

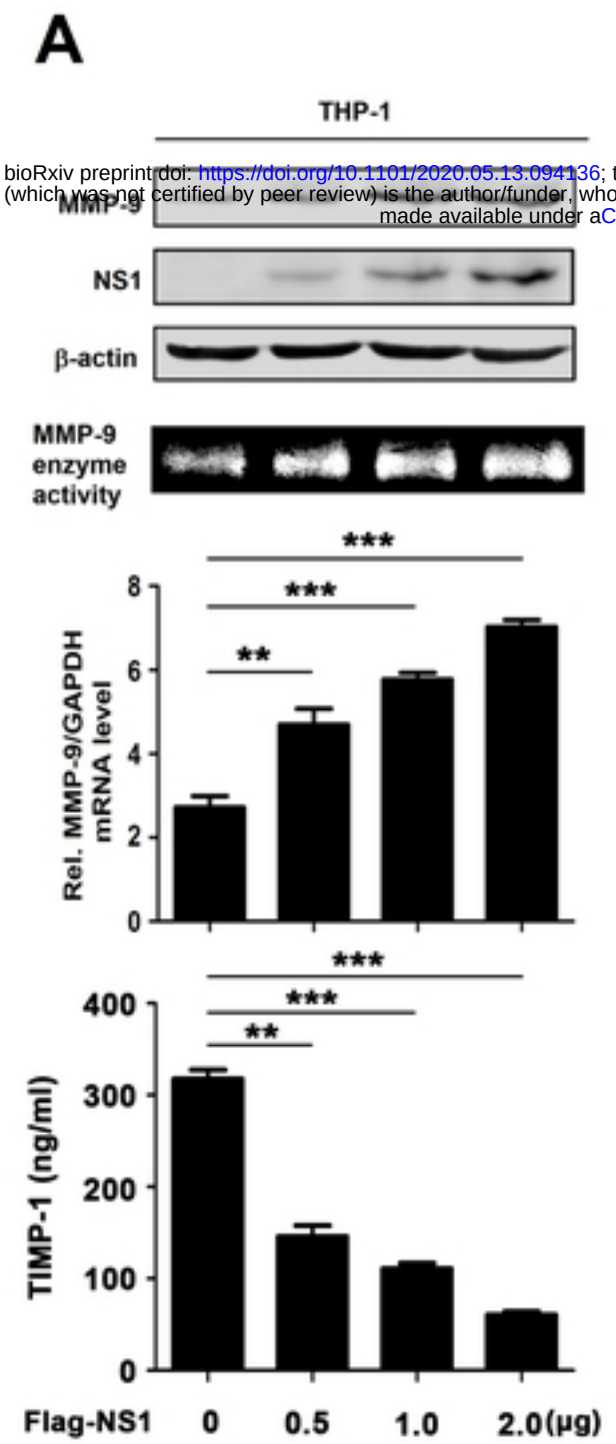

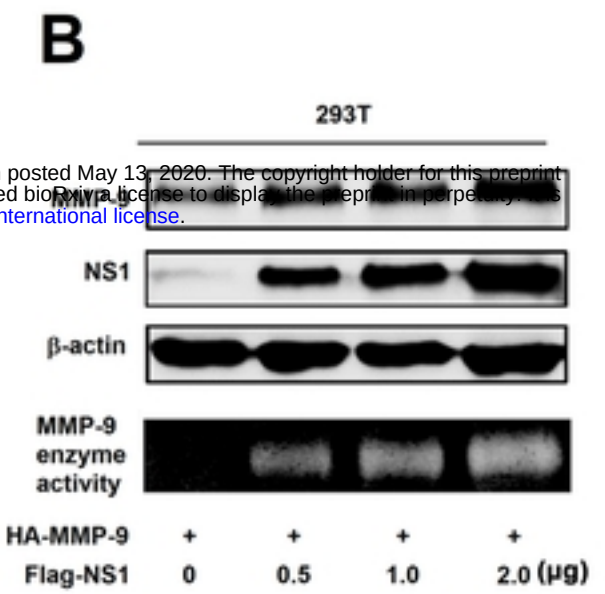

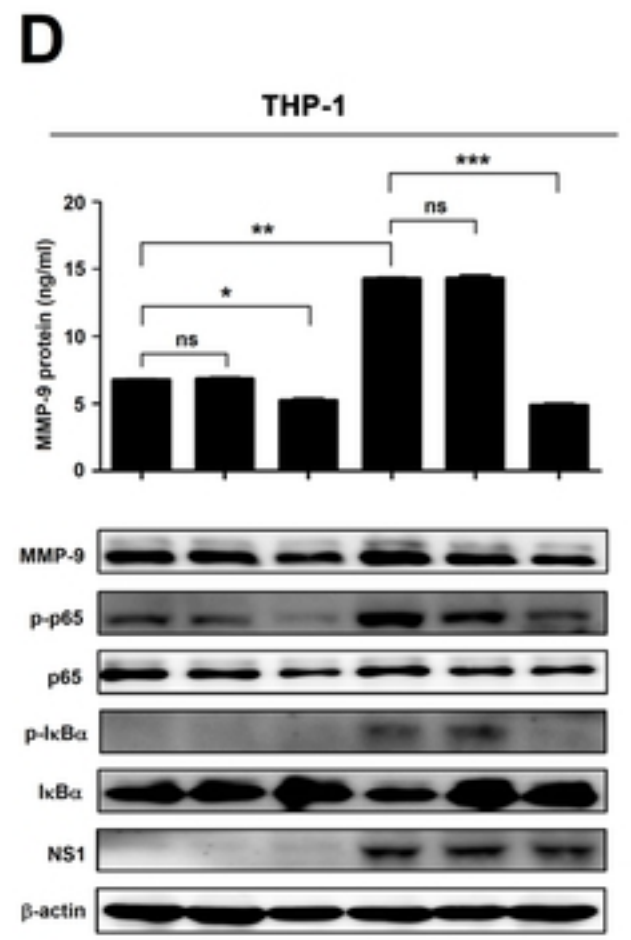

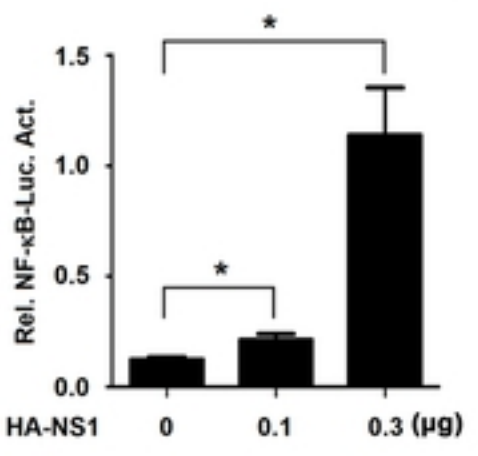

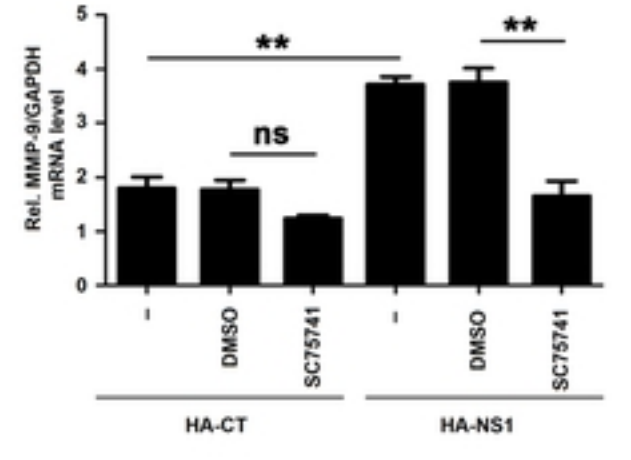

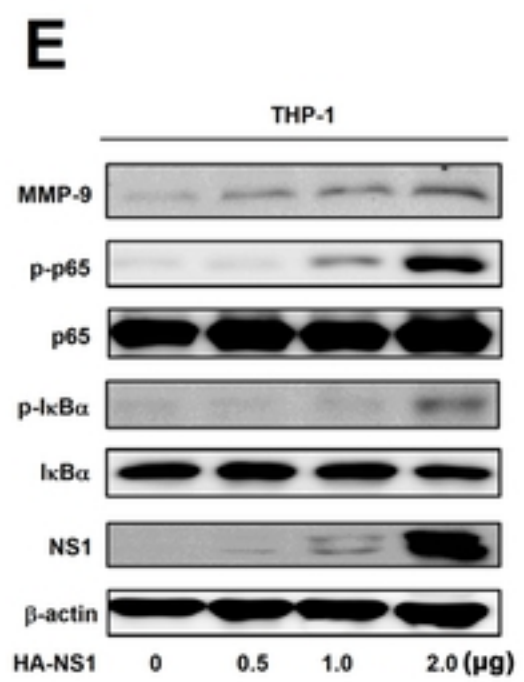

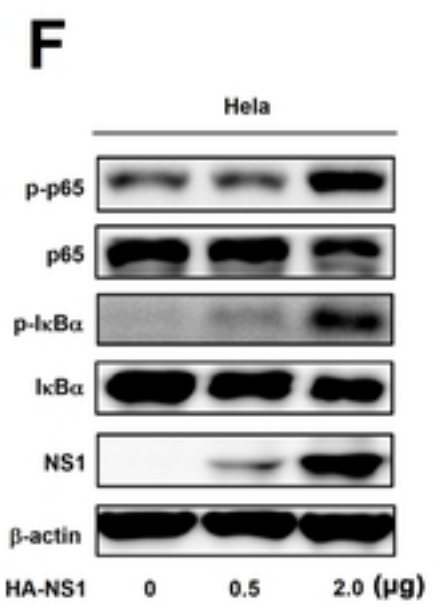

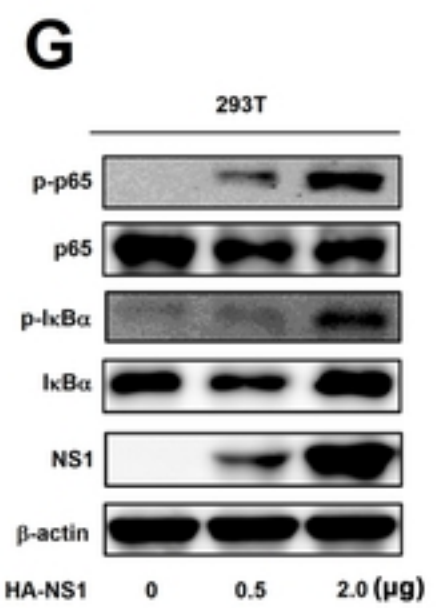

Figure 3

Figure 4

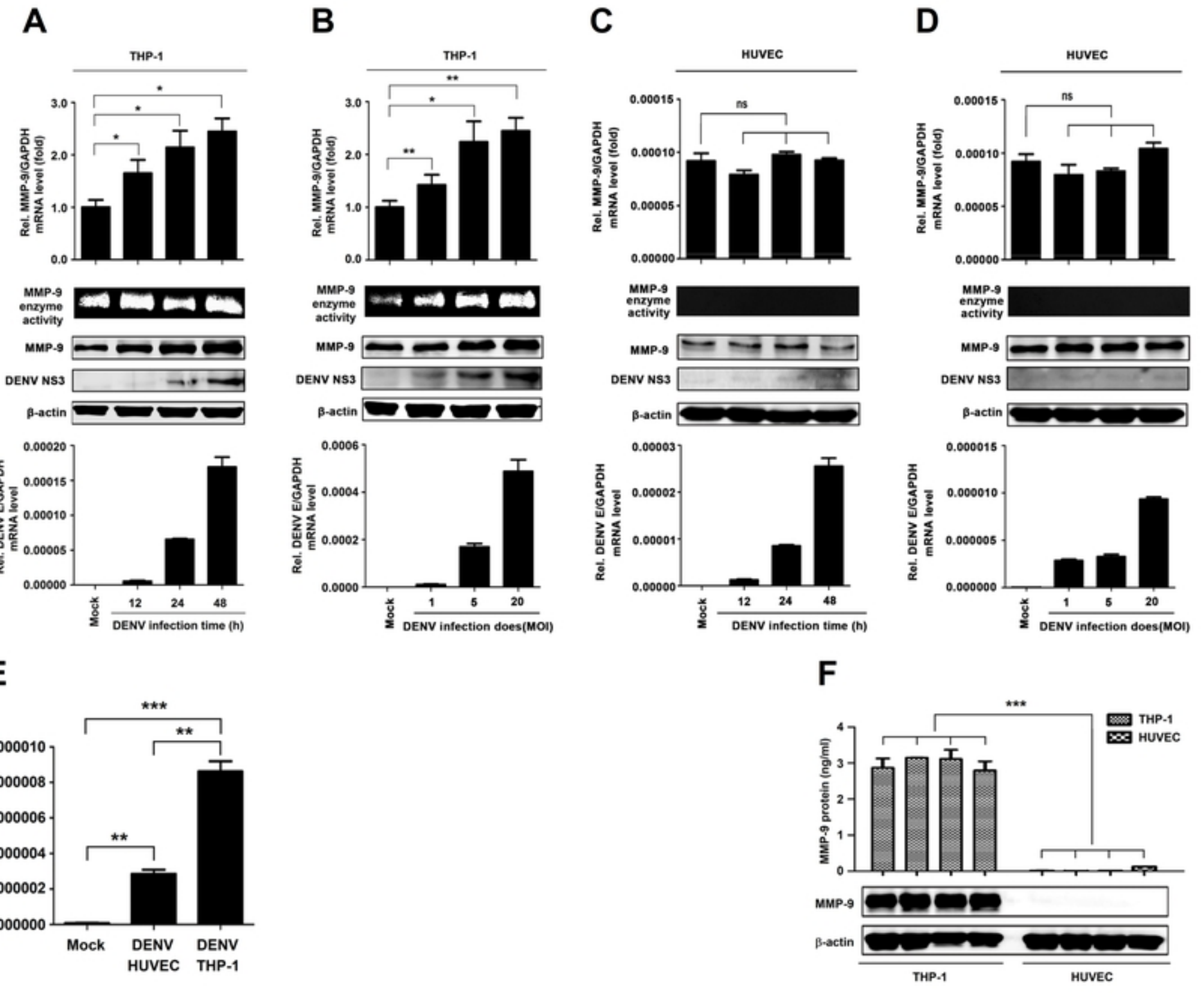

Figure 4

Figure 5

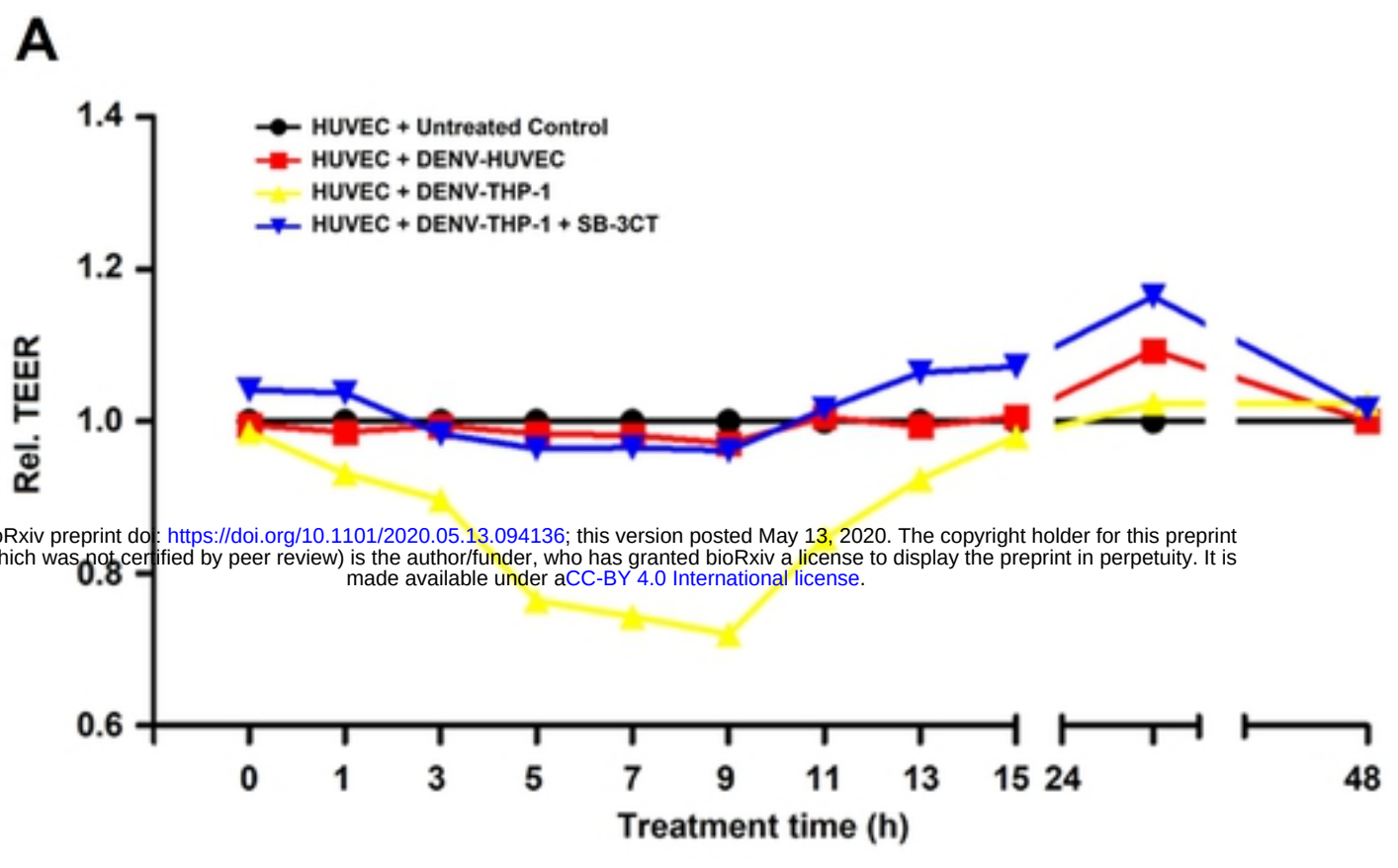

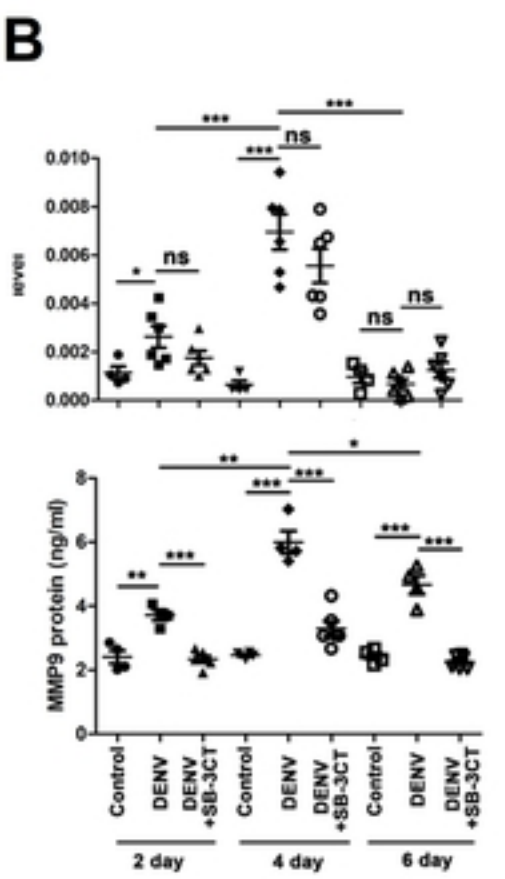

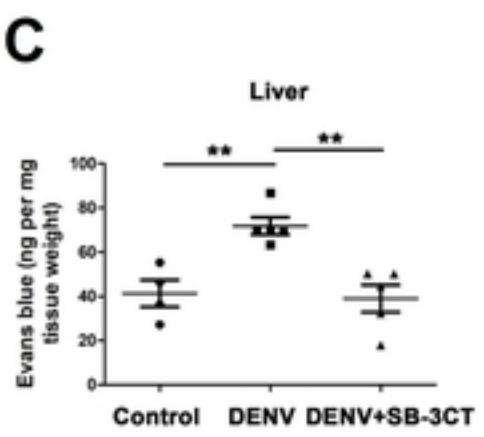

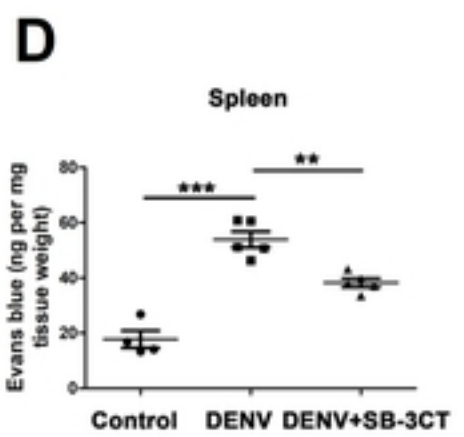

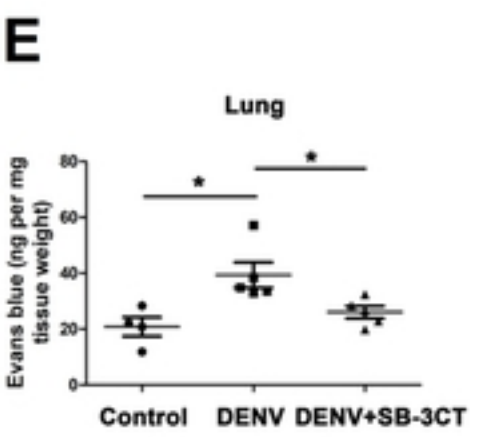

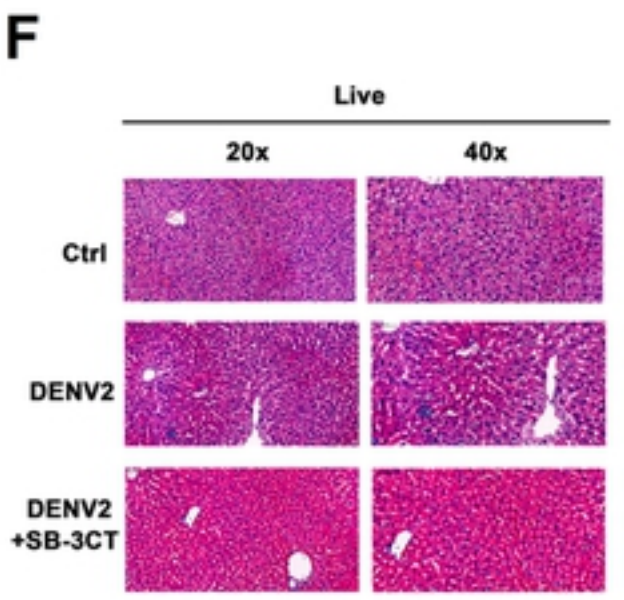

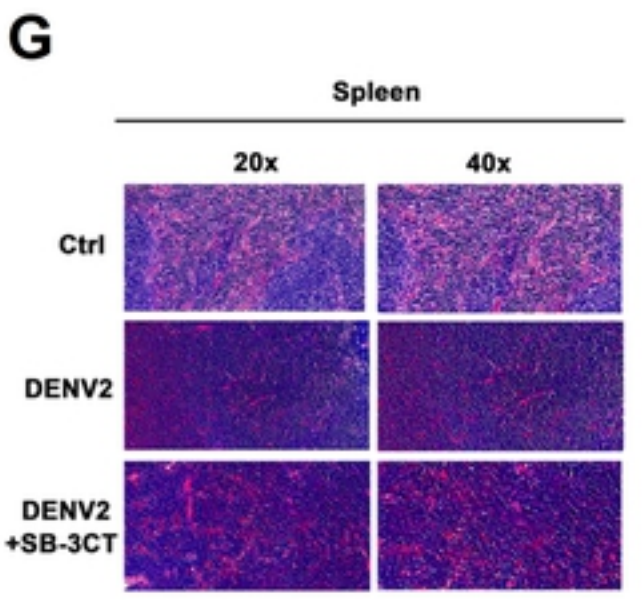

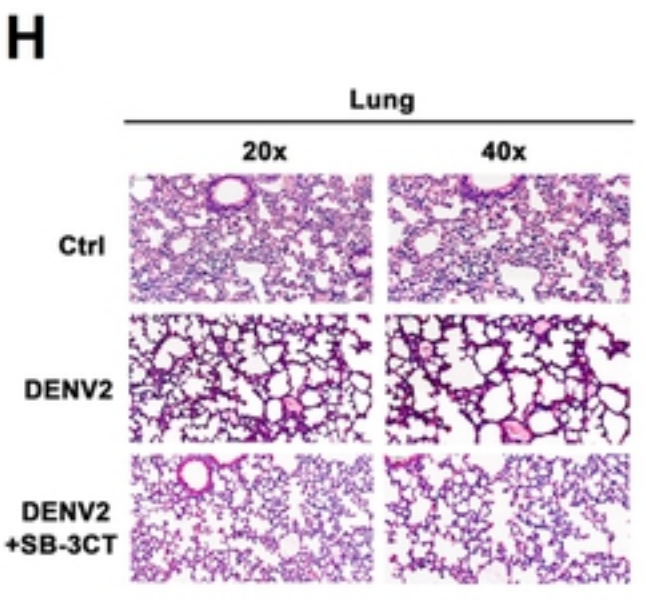

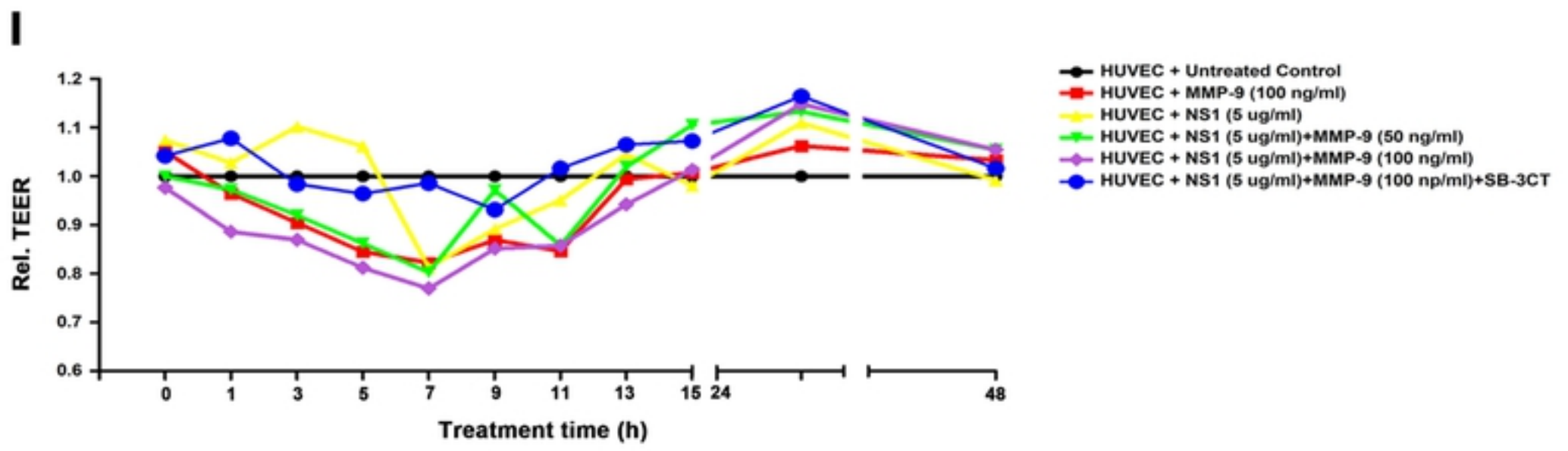

Figure 5

Figure 6

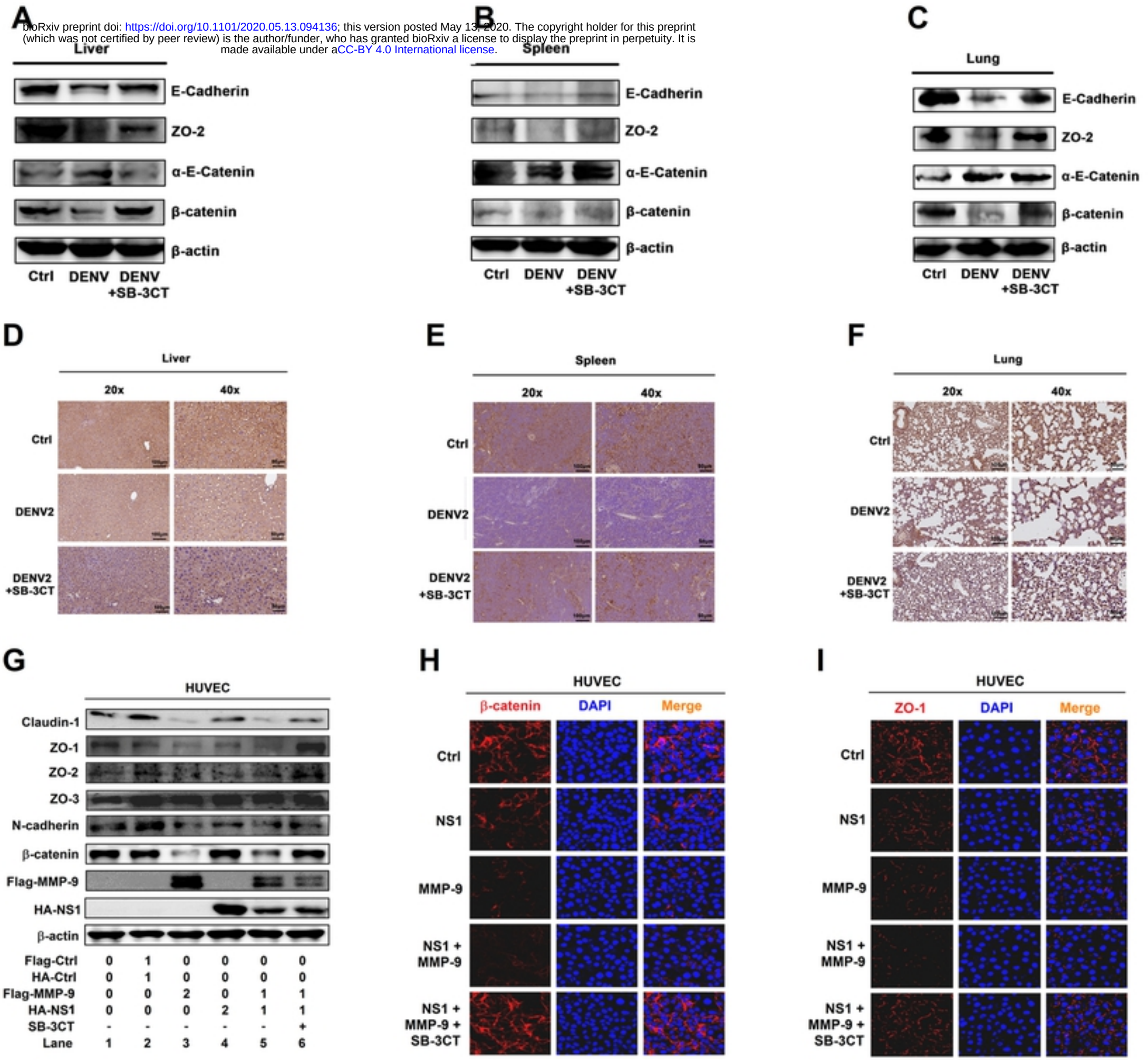

Figure 6

Figure 7

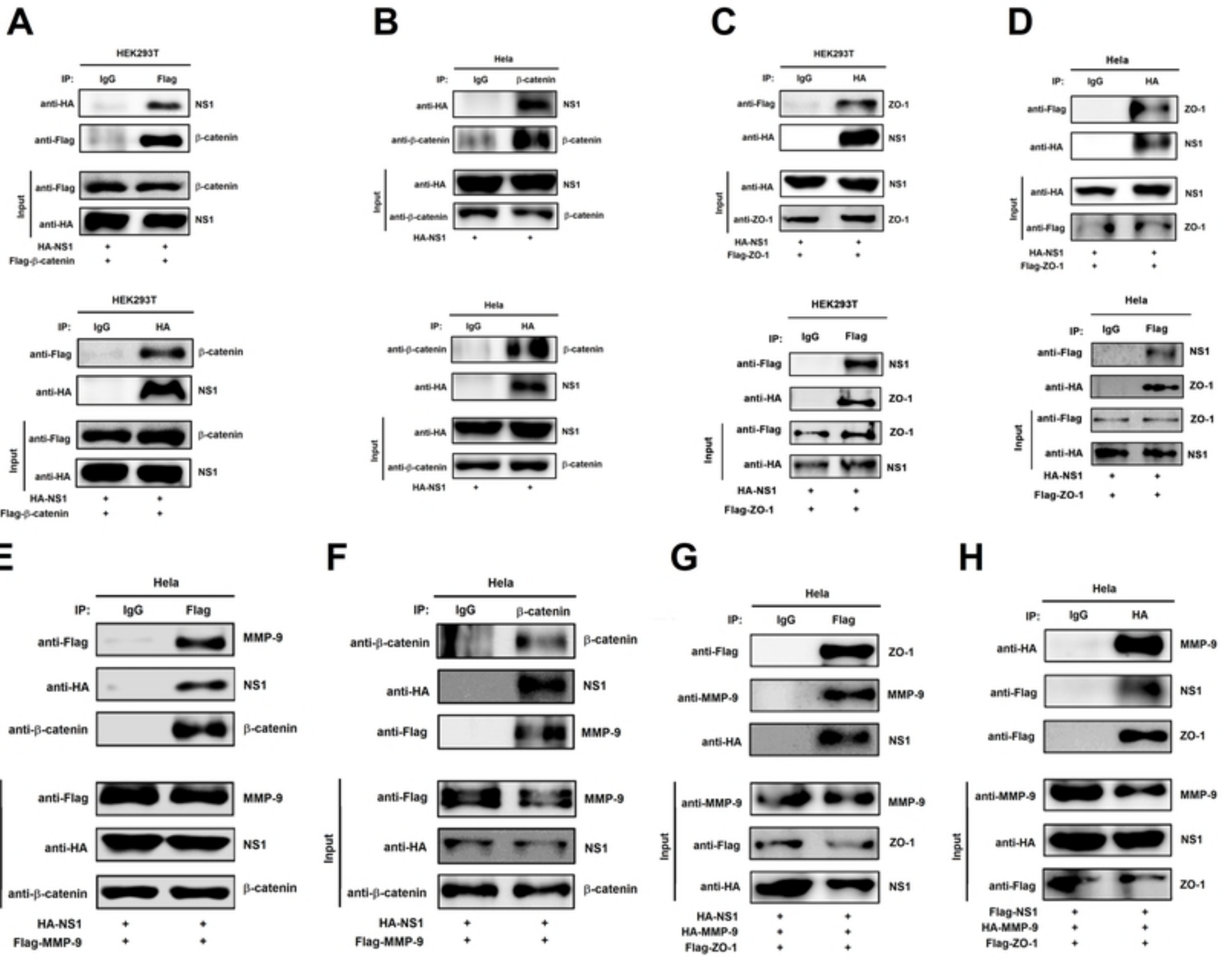

Figure 7

Figure 8

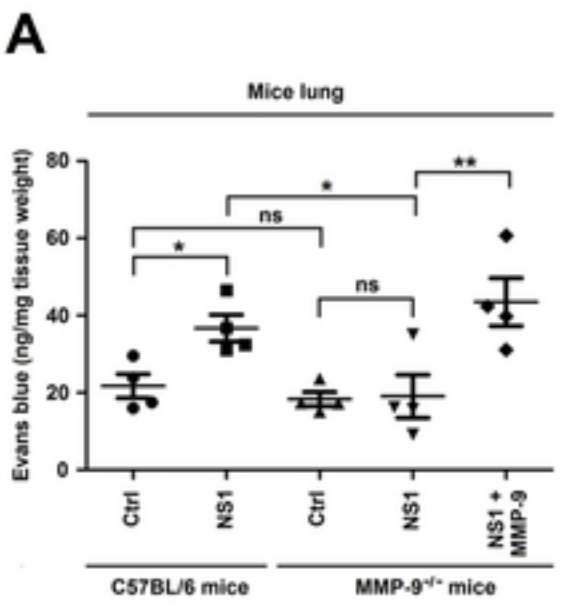

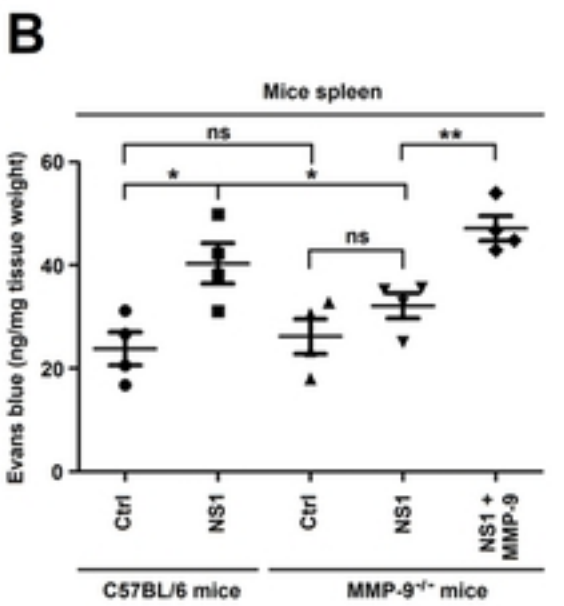

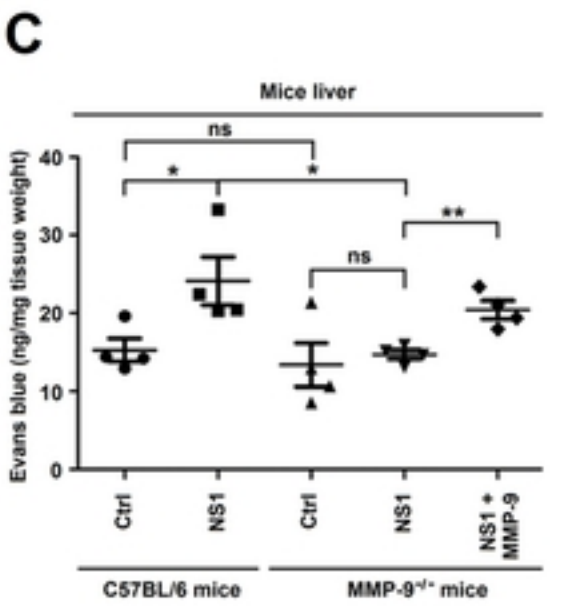

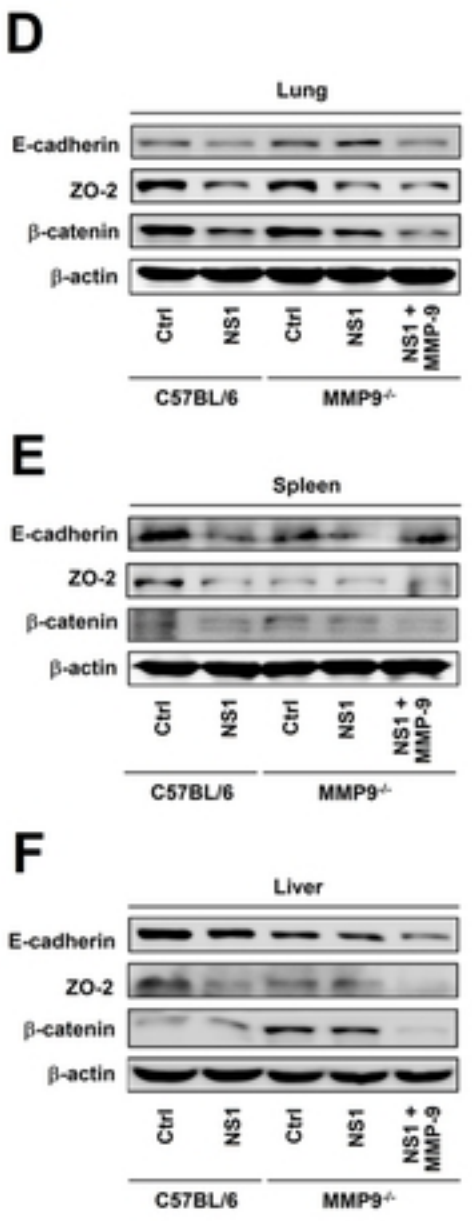

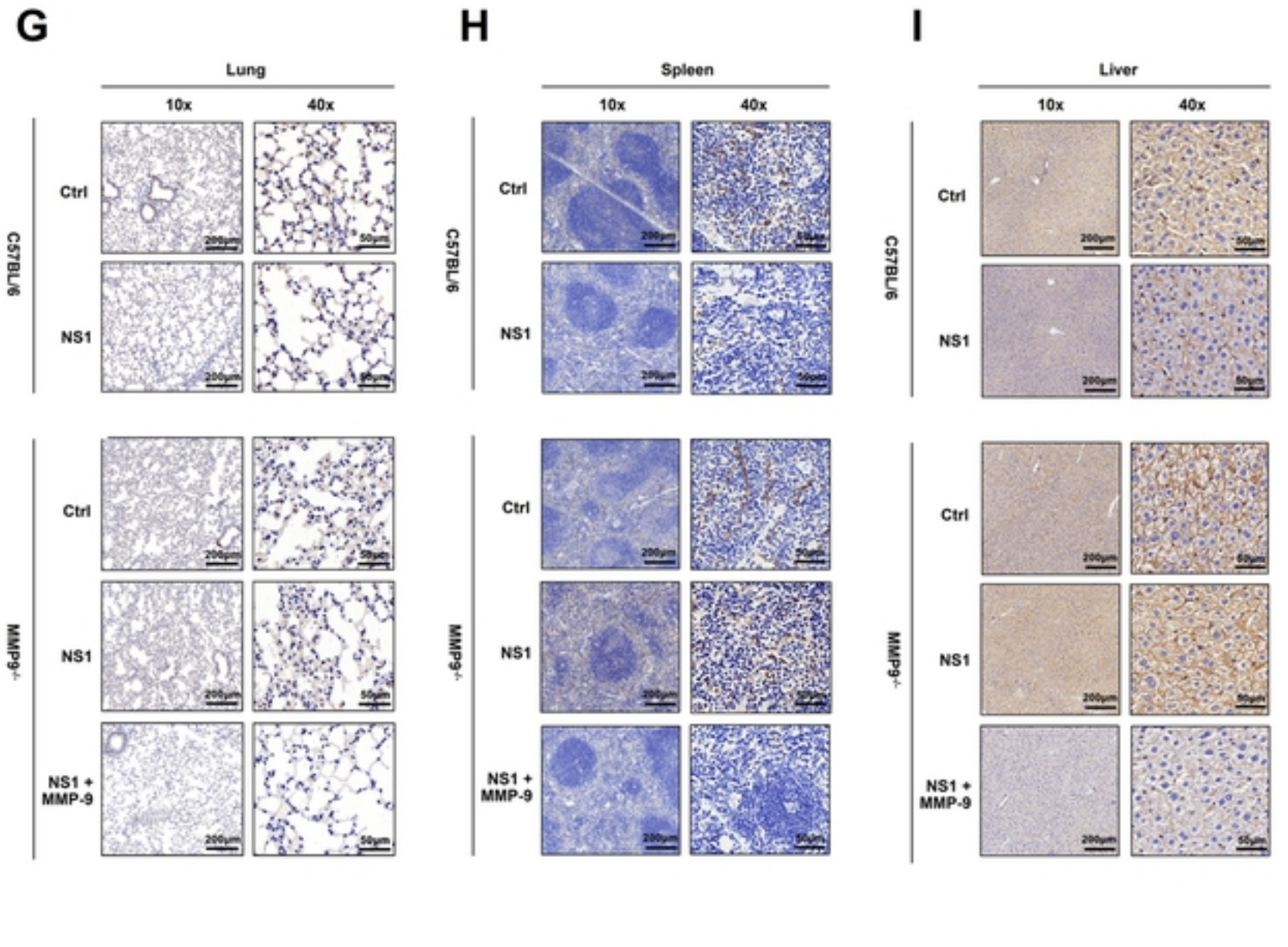

Figure 8

Figure 9

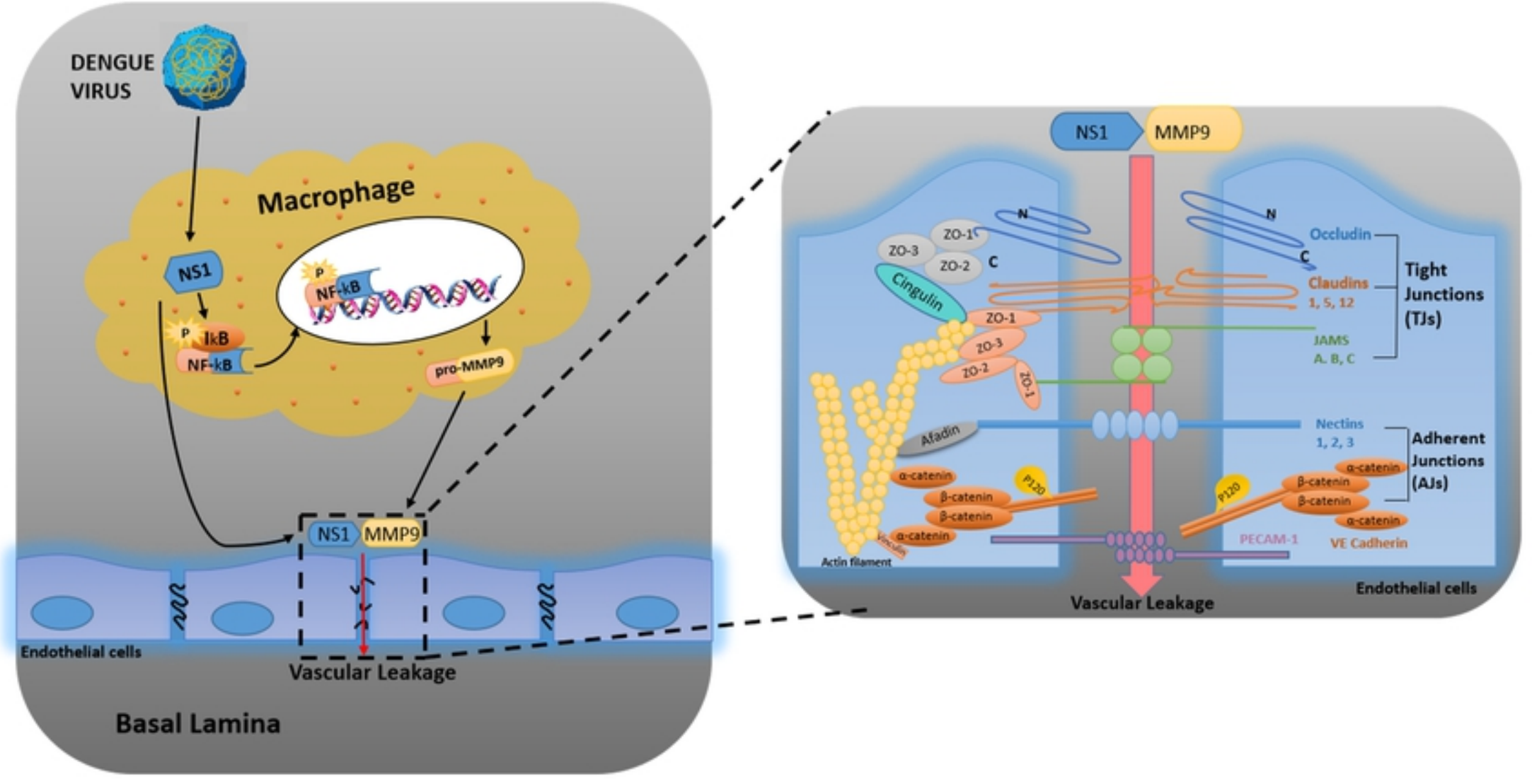

Figure 9